A priori and a posteriori error analyses of an HDG method for the Brinkman problem *

Luis F. Gatica† Filánder A. Sequeira‡

Abstract

In this paper we introduce and analyze a hybridizable discontinuous Galerkin (HDG) method for the linear Brinkman model of porous media flow in two and three dimensions, with non-homogeneous Dirichlet boundary conditions. We consider a fully-mixed formulation in which the main unknowns are given by the pseudostress, the velocity and the trace of the velocity, whereas the pressure is easily recovered through a simple postprocessing. We show that the corresponding continuous and discrete schemes are well-posed. In particular, we use the projection-based error analysis in order to derive *a priori* error estimates. Furthermore, we develop a reliable and efficient residual-based *a posteriori* error estimator, and propose the associated adaptive algorithm for our HDG approximation. Finally, several numerical results illustrating the performance of the method, confirming the theoretical properties of the estimator, and showing the expected behaviour of the adaptive refinements are presented.

Key words: linear Brinkman model, hybridized discontinuous Galerkin method, a posteriori error analysis, postprocessed techniques, high-order approximations

1 Introduction

The design and study of efficient numerical methods to solving the Brinkman model, which describes the flow of a viscous fluid in a highly porous medium, has been increasing during the last few years (see, e.g., [1, 2, 3, 4, 19, 21, 23, 30, 31, 32, 33, 36] and the references therein). The reason why it has gained relevance on the part of the numerical analysis community is due to its various applications (see, e.g. [30] and the references therein) including for instance, subsurface flow problems, heat and mass transfer in pipes, liquid composite molding, the behavior and influence of osteonal structures, computational fuel cell dynamics, to name a few. This model is also encountered after time discretizations of transient Stokes equations governing the motion of an incompressible fluid. Since we are mainly interested in mixed variational formulations, we note that most of the variational formulations found in the literature are based on the typical Stokes-type (also called primal-mixed) approach in which the velocity and the pressure are kept as the main unknowns. Actually, up to the authors' knowledge, no stress-based or pseudostress-based approaches seemed to be available until the recent contribution [21], where an alternative way of dealing with the mixed boundary conditions and the *a priori* and *a posteriori* error analyses of a dual-mixed approach for the two-dimensional Brinkman problem were

*This work of the first author was partially supported by Dirección de Investigación of the Universidad Católica de la Santísima Concepción, Chile, through the project DIN 14/2016.

†Departamento de Matemática y Física Aplicadas, Facultad de Ingeniería, Universidad Católica de la Santísima Concepción, Casilla 297, and CI^{2}MA - Universidad de Concepción, Casilla 160-C, Concepción, Chile, email: lgatica@ucsc.cl

‡Escuela de Matemática, Universidad Nacional, Campus Omar Dengo, Heredia, Costa Rica, email: filander.sequeira@una.cr

provided. Indeed, the pseudostress $\boldsymbol{\sigma}$ is the main unknown of the resulting saddle point problem in [21], and the velocity and pressure are easily recovered in terms of $\boldsymbol{\sigma}$ through simple postprocessing formulae. In addition, as it is usual for dual-mixed methods, the Dirichlet boundary condition for the velocity becomes natural in this case, and the Neumann boundary condition, being essential, is imposed weakly through the introduction of the trace of the velocity on that boundary as the associated Lagrange multiplier. In this way, the Babuška-Brezzi theory is applied first in [21] to establish sufficient conditions for the well-posedness of the resulting continuous and discrete formulations. In particular, a feasible choice of finite element subspaces is given by Raviart-Thomas elements of order $k \geq 0$ for the pseudostress, and continuous piecewise polynomials of degree $k+1$ for the Lagrange multiplier. Next, a reliable and efficient residual-based *a posteriori* error estimator is derived there. Suitable auxiliary problems, the continuous inf-sup conditions satisfied by the bilinear forms involved, a discrete Helmholtz decomposition, and the local approximation properties of the Raviart-Thomas and Clément interpolation operators are the main tools for proving the reliability. In turn, Helmholtz's decomposition, inverse inequalities, and the localization technique based on triangle-bubble and edge-bubble functions are employed to show the efficiency. Lately, a natural extension of the analysis and results from [21] to a class of Brinkman models whose viscosity depends nonlinearly on the gradient of the velocity, which is a characteristic feature of quasi-Newtonian Stokes flows, was developed in [23]. A reliable and efficient residual-based *a posteriori* error estimator was also derived in [23] by following basically the same approach from [21]. More recently, also proceeding as in [21], an *a priori* error analysis of a mixed virtual element method (mixed-VEM) approach for the two-dimensional Brinkman problem with non-homogeneous Dirichlet boundary conditions was developed in [4].

On the other hand, the hybridizable discontinuous Galerkin (HDG) method, introduced in [10] for diffusion problems, is one of the several high-order discretization schemes that takes advantage from the hybridization technique originally applied in [17] to the local discontinuous Galerkin (LDG) method for time dependent convection-diffusion problems. The main advantages of HDG methods include a substantial reduction of the globally coupled degrees of freedom, and the fact that convergence is obtained even for the polynomial degree $k = 0$. Additionally, superconvergence element-by-element postprocessing techniques can be also develop for this approach (see e.g. ([9, 13, 11]). In the context of the Stokes-type equations, the hybridization for DG methods was initially introduced in [5] and then analyzed in [34, 11]. Lately, an overview of the recent work by Cockburn and co-workers on the devising of HDG methods for the Stokes equations of incompressible flow was provided in [16]. More recently, *a priori* and *a posteriori* error analyses of augmented HDG method for a quasi-Newtonian Stokes flow are developed in [27] (see also [26]), and in [28] the authors introduce and analyze a HDG method for numerically solving the coupling of fluid flow with porous media flow, governing by the Stokes and Darcy equations, respectively. Nevertheless, and up to our knowledge, there is just the contribution [19] in the literature concerning HDG for Brinkman systems. Therein, two new parameter-free superconvergent $H(\mathrm{div})$-conforming HDG methods are presented for the Brinkman equations on both simplicial and rectangular meshes. The methods are based on a velocity gradient-velocity-pressure formulation, which can be considered as a natural extension of the $H(\mathrm{div})$-conforming HDG method for the Stokes flow from [14].

According to the above discussion, in this paper we are interested in applying the HDG approach to the two and three dimensional lineal Brinkman problem with non-homogeneous Dirichlet boundary conditions studied in [4], using the same velocity-pseudostress formulation from [22] (see also [4]) for the corresponding *a priori* error analysis. Furthermore, a second contribution of this work corresponds to the derivation of a reliable and efficient residual-based *a posteriori* error estimator for our problem. Regarding this issue, it is important to remark here that the development of *a posteriori* error analysis for HDG schemes is not as exhaustive as for conforming methods, which is confirmed by the scarce literature on the subject. One of the first *a posteriori* error analysis of the HDG method for second-order elliptic problems was presented in [18]. A postprocessing variable was used there in order

to prove reliability and efficiency of the proposed local *a posteriori* error indicator. More recently, an *a posteriori* error estimator for the HDG method applied to convection-diffusion equations with dominant convection was introduced in [6]. No postprocessed solution was employed in that approach. Other works dealing with the development of *a posteriori* error estimates for HDG schemes include [27], where an element-by-element postprocessing formula for the pseudostress was used, in order to provide reliability and efficiency of the *a posteriori* estimator. However, in spite of the aforementioned papers, there is still no contribution available in the literature on the *a posteriori* error analysis of HDG methods for Brinkman models. For all the reasons above, and as a first attempt in this regard, in this paper we follow [27] and develop a reliable and efficient residual-based *a posteriori* error estimator, and propose the associated adaptive algoritm for our HDG approximation of the linear Brinkman problem.

The rest of this work is organized as follows. In Section 2 we introduce the boundary value problem of interest, and analyze its pseudostress-velocity formulation. Next, in Section 3 we follow [26, 27] to establish a hybridizable discontinuous Galerkin formulation, which involves the pseudostress, the velocity, and the trace of the velocity as main unknowns. Also, in the same section, we show the unique solvability of this HDG scheme, and establish the corresponding optimal *a priori* error estimates. Therein, we use a projection whose design is inspired by the form of the numerical traces of the method, which has the task of simplifying the corresponding study. Next, in Section 4 we derive a reliable and efficient residual-based *a posteriori* error estimator. Similarly as in [18, 27], we use an element-by-element postprocessing formula for the pseudostress, which allows us to prove reliability and efficiency of the *a posteriori* estimator. Finally, several numerical results showing the good performance of the method, confirming the reliability and efficiency of the estimator, and illustrating the behaviour of the associated adaptive algorithm are reported in Section 5, even for $k = 0$, which is a polynomial degree not fully covered by the theory.

We end the present section by describing the notational convention to be used below. Given a non-null space H and $n \in \{2, 3\}$, we set $\mathbf{H} := H^n$ and $\mathbb{H} := H^{n\times n}$. Also, given $\boldsymbol{\tau} := (\tau_{ij})$, $\boldsymbol{\zeta} := (\zeta_{ij}) \in \mathrm{R}^{n\times n}$, we write as usual

$$\boldsymbol{\tau}^{\mathtt{t}} := (\tau_{ji}), \quad \mathrm{tr}(\boldsymbol{\tau}) := \sum_{i=1}^{n} \tau_{ii}, \quad \boldsymbol{\tau}^{\mathrm{d}} := \boldsymbol{\tau} - \frac{1}{n}\mathrm{tr}(\boldsymbol{\tau})\,\mathbb{I}, \quad \text{and} \quad \boldsymbol{\tau} : \boldsymbol{\zeta} := \sum_{i,j=1}^{n} \tau_{ij}\zeta_{ij}.$$

Furthermore, in what follows we utilize the standard terminology for Sobolev spaces and norms, and use C to denote generic constants independent of the discretization parameters, which may take different values at different places.

2 The continuous problem

Let Ω be a bounded and simply connected polygonal domain in R^n, $n \in \{2, 3\}$, with boundary Γ. Our goal is to determine the velocity $\mathbf{u}$, the pseudostress $\boldsymbol{\sigma}$, and the pressure p of a steady flow occupying the region Ω. In other words, given a volume force $\mathbf{f} \in \mathbf{L}^2(\Omega)$ and a Dirichlet datum $\mathbf{g} \in \mathbf{H}^{1/2}(\Gamma)$, we seek a tensor field $\boldsymbol{\sigma}$, a vector field $\mathbf{u}$ and a scalar field p such that

$$\begin{aligned} \boldsymbol{\sigma} &= \nu\,\nabla\mathbf{u} - p\,\mathbb{I} \quad \text{in } \Omega, \qquad \alpha\,\mathbf{u} - \mathbf{div}(\boldsymbol{\sigma}) = \mathbf{f} \quad \text{in } \Omega, \\ \mathrm{div}(\mathbf{u}) &= 0 \quad \text{in } \Omega, \qquad \mathbf{u} = \mathbf{g} \quad \text{on } \Gamma, \quad \text{and} \quad \int_\Omega p = 0, \end{aligned} \tag{2.1}$$

where $\nu > 0$ is the dynamic viscosity, and $\alpha > 0$ is a constant approximation of the viscosity divided by the permeability. In addition, as required by the incompressibility condition, we assume from now on that the datum $\mathbf{g}$ satisfies the compatibility condition $\int_\Gamma \mathbf{g}\cdot\boldsymbol{n} = 0$, where $\boldsymbol{n}$ stands for the unit

outward normal at Γ. Furthermore, the incompressible condition also implies that the formulation (2.1) can be rewritten as:

$$\begin{aligned} \frac{1}{\nu}\,\boldsymbol{\sigma}^{\mathrm{d}} \;&=\; \nabla\mathbf{u} \quad \text{in } \Omega\,, \quad \alpha\,\mathbf{u} - \mathbf{div}(\boldsymbol{\sigma}) \;=\; \mathbf{f} \quad \text{in } \Omega\,, \\ \mathbf{u} \;&=\; \mathbf{g} \quad \text{on } \Gamma\,, \quad \text{and} \quad \int_\Omega \mathrm{tr}(\boldsymbol{\sigma}) \;=\; 0\,, \end{aligned} \tag{2.2}$$

where, the pressure p can be obtained by the postprocessing formula

$$p \;=\; -\frac{1}{n}\,\mathrm{tr}(\boldsymbol{\sigma}) \quad \text{in } \Omega\,. \tag{2.3}$$

Now, we test the first and second equations of (2.2) with $\boldsymbol{\tau} \in \mathbb{H}(\mathbf{div};\Omega)$ and $\mathbf{v} \in \mathbf{L}^2(\Omega)$, respectively. Then, integrating by parts the expression $\int_\Omega \nabla\mathbf{u} : \boldsymbol{\tau}$, and using the Dirichlet boundary condition, we obtain the variational formulation: Find $(\boldsymbol{\sigma},\mathbf{u}) \in \mathbb{H} \times \mathbf{Q}$ such that

$$\begin{aligned} \frac{1}{\nu}\int_\Omega \boldsymbol{\sigma}^{\mathrm{d}} : \boldsymbol{\tau}^{\mathrm{d}} \;+\; \int_\Omega \mathbf{u}\cdot\mathbf{div}(\boldsymbol{\tau}) \;&=\; \langle \boldsymbol{\tau}\boldsymbol{n}, \mathbf{g}\rangle_\Gamma \qquad \forall\, \boldsymbol{\tau} \in \mathbb{H}\,, \\ \int_\Omega \mathbf{v}\cdot\mathbf{div}(\boldsymbol{\sigma}) \;-\; \alpha\int_\Omega \mathbf{u}\cdot\mathbf{v} \;&=\; -\int_\Omega \mathbf{f}\cdot\mathbf{v} \qquad \forall\, \mathbf{v} \in \mathbf{Q}\,, \end{aligned} \tag{2.4}$$

where $\mathbb{H} := \mathbb{H}_0(\mathbf{div};\Omega) := \big\{\boldsymbol{\tau} \in \mathbb{H}(\mathbf{div};\Omega) \,:\, \int_\Omega \mathrm{tr}(\boldsymbol{\tau}) \,=\, 0\big\}$, and $\mathbf{Q} := \mathbf{L}^2(\Omega)$. The unique solvability of (2.4) is established in the following result.

Theorem 2.1. *Assume that* $\mathbf{f} \in \mathbf{L}^2(\Omega)$ *and* $\mathbf{g} \in \mathbf{H}^{1/2}(\Gamma)$. *Then, there exists a unique solution* $(\boldsymbol{\sigma},\mathbf{u}) \in \mathbb{H} \times \mathbf{Q}$ *to* (2.4). *In addition, there exists* $C > 0$ *such that*

$$\|\boldsymbol{\sigma}\|_{\mathbf{div},\Omega} \;+\; \|\mathbf{u}\|_{0,\Omega} \;\leq\; C\,\Big\{\|\mathbf{f}\|_{0,\Omega} \;+\; \|\mathbf{g}\|_{1/2,\Gamma}\Big\}\,. \tag{2.5}$$

Proof. First, we derive an equivalent formulation for (2.4). Indeed, taking $\mathbf{v} := \mathbf{div}(\boldsymbol{\sigma}) - \alpha\,\mathbf{u} + \mathbf{f} \in \mathbf{L}^2(\Omega)$ in the second equation of (2.4), we deduce that

$$\mathbf{u} \;=\; \frac{1}{\alpha}\,\big\{\mathbf{f} \;+\; \mathbf{div}(\boldsymbol{\sigma})\big\} \quad \text{in } \Omega\,. \tag{2.6}$$

Next, replacing $\mathbf{u}$ in the first equation of (2.4) by (2.6) lead to the problem: Find $\boldsymbol{\sigma} \in \mathbb{H}$ such that

$$\frac{1}{\nu}\int_\Omega \boldsymbol{\sigma}^{\mathrm{d}} : \boldsymbol{\tau}^{\mathrm{d}} \;+\; \frac{1}{\alpha}\int_\Omega \mathbf{div}(\boldsymbol{\sigma})\cdot\mathbf{div}(\boldsymbol{\tau}) \;=\; -\frac{1}{\alpha}\int_\Omega \mathbf{f}\cdot\mathbf{div}(\boldsymbol{\tau}) \;+\; \langle \boldsymbol{\tau}\boldsymbol{n}, \mathbf{g}\rangle_\Gamma \quad \forall\, \boldsymbol{\tau} \in \mathbb{H}\,,$$

which, is quite clear (see, e.g. [4, Section 2]) that there exists a unique solution $\boldsymbol{\sigma} \in \mathbb{H}$ of the above formulation (which is equivalent to (2.4)). In addition, we have that

$$\|\boldsymbol{\sigma}\|_{\mathbf{div},\Omega} \;\leq\; C\,\Big\{\|\mathbf{f}\|_{0,\Omega} \;+\; \|\mathbf{g}\|_{1/2,\Gamma}\Big\}\,. \tag{2.7}$$

Finally, from (2.6) we know that $\|\mathbf{u}\|_{0,\Omega} \leq \frac{1}{\alpha}\big\{\|\mathbf{f}\|_{0,\Omega} + \|\boldsymbol{\sigma}\|_{\mathbf{div},\Omega}\big\}$, which along with (2.7), allows ut to conclude (2.5) and complete the proof. □

We end this section by noting from Theorem 2.1 that the bounded linear operator $\mathcal{A} : \mathbb{H} \times \mathbf{Q} \to \mathbb{H}' \times \mathbf{Q}'$, obtained by adding the two equations of the left-hand side of (2.4), is an isomorphism. This means, in particular, according to (2.5), that there exists $C > 0$, depending on Ω, ν and α, such that

$$\|\mathcal{A}(\boldsymbol{\rho},\mathbf{w})\|_{\mathbb{H}'\times\mathbf{Q}'} \;\geq\; C\,\|(\boldsymbol{\rho},\mathbf{w})\|_{\mathbb{H}\times\mathbf{Q}} \qquad \forall\, (\boldsymbol{\rho},\mathbf{w}) \in \mathbb{H} \times \mathbf{Q}\,,$$

which can be written, equivalently, as a global inf-sup condition. More precisely, there exists a constant $C > 0$ such that

$$C \, \|(\boldsymbol{\rho}, \mathbf{w})\|_{\mathbb{H}\times\mathbf{Q}} \;\leq\; \sup_{\substack{(\boldsymbol{\tau},\mathbf{v})\in\mathbb{H}\times\mathbf{Q} \\ (\boldsymbol{\tau},\mathbf{v})\neq\mathbf{0}}} \frac{\frac{1}{\nu}\int_\Omega \boldsymbol{\rho}^{\mathrm{d}} : \boldsymbol{\tau}^{\mathrm{d}} \,+\, \int_\Omega \mathbf{w}\cdot\mathbf{div}(\boldsymbol{\tau}) \,+\, \int_\Omega \mathbf{v}\cdot\mathbf{div}(\boldsymbol{\rho}) \,-\, \alpha\int_\Omega \mathbf{w}\cdot\mathbf{v}}{\|(\boldsymbol{\tau},\mathbf{v})\|_{\mathbb{H}\times\mathbf{Q}}} \tag{2.8}$$

for all $(\boldsymbol{\rho}, \mathbf{w}) \in \mathbb{H}\times\mathbf{Q}$. The purpose of (2.8) will become clear in the *a posteriori* error analysis given below in Section 4.

3 The hybridizable discontinuous Galerkin method

We begin by introducing some preliminary notations. Let $\mathcal{T}_h$ be a shape-regular triangulation of $\overline{\Omega}$ without the presence of hanging nodes, and let $\mathcal{E}_h$ be the set of faces F of $\mathcal{T}_h$. In addition, we let $\mathcal{E}_h^i$ and $\mathcal{E}_h^\partial$ be the set of interior and boundary faces, respectively, of $\mathcal{E}_h$, and set $\partial\mathcal{T}_h := \cup\{\partial T \,:\, T\in\mathcal{T}_h\}$. Next, given a domain $U \subseteq \mathrm{R}^n$ and a surface $G \subseteq \mathrm{R}^{n-1}$, we let $(\cdot,\cdot)_U$ (resp. $\langle\cdot,\cdot\rangle_G$) be the usual L^2, $\mathbf{L}^2$ and $\mathbb{L}^2$ (resp. L^2 and $\mathbf{L}^2$) inner products over U (resp. G). Then, we introduce the inner products:

$$(\cdot,\cdot)_{\mathcal{T}_h} \;:=\; \sum_{T\in\mathcal{T}_h}(\cdot,\cdot)_T\,, \quad \langle\cdot,\cdot\rangle_{\partial\mathcal{T}_h} \;:=\; \sum_{T\in\mathcal{T}_h}\langle\cdot,\cdot\rangle_{\partial T}\,, \quad \text{and} \quad \langle\cdot,\cdot\rangle_{\partial\mathcal{T}_h\backslash\Gamma} \;:=\; \sum_{T\in\mathcal{T}_h}\sum_{F\in\partial T\backslash\Gamma}\langle\cdot,\cdot\rangle_F\,.$$

On the other hand, let $\boldsymbol{n}^+$ and $\boldsymbol{n}^-$ be the outward unit normal vectors on the boundaries of two neighboring elements T^+ and T^-, respectively. We use $\boldsymbol{\tau}^\pm$ to denote the traces of $\boldsymbol{\tau}$ on $F := \overline{T}^+\cap\overline{T}^-$ from the interior of $T^\pm$, where $\boldsymbol{\tau}$ is a second-order tensorial function. Then, we define the jumps $[\![\cdot]\!]$ of tensor variables on each interior face as $[\![\boldsymbol{\tau}\boldsymbol{n}]\!] := \boldsymbol{\tau}^+\boldsymbol{n}^+ + \boldsymbol{\tau}^-\boldsymbol{n}^-$. In addition, given an integer $\ell \geq 0$, we denote by $\mathrm{P}_\ell(U)$ the space of polynomials defined in U of total degree at most ℓ. We recall here, according to our notations (see the last paragraph of Section 1), that $\mathbf{P}_\ell(U) := [\mathrm{P}_\ell(U)]^n$ and $\mathbb{P}_\ell(U) := [\mathrm{P}_\ell(U)]^{n\times n}$.

We are now ready to describe below the HDG method for the boundary value problem (2.2). To this end, given an integer $k \geq 0$, we introduce the finite dimensional discontinuous subspaces given by

$$\begin{aligned}
\mathbb{H}_h &:= \Big\{\boldsymbol{\tau}\in\mathbb{L}^2(\Omega) \,:\, \boldsymbol{\tau}|_T\in\mathbb{P}_k(T) \quad \forall\, T\in\mathcal{T}_h\Big\}\,,\\
\mathbf{Q}_h &:= \Big\{\mathbf{v}\in\mathbf{L}^2(\Omega) \,:\, \mathbf{v}|_T\in\mathbf{P}_k(T) \quad \forall\, T\in\mathcal{T}_h\Big\}\,,\\
\mathbf{M}_h &:= \Big\{\boldsymbol{\mu}\in\mathbf{L}^2(\mathcal{E}_h^i) \,:\, \boldsymbol{\mu}|_F\in\mathbf{P}_k(F) \quad \forall\, F\in\mathcal{E}_h^i\Big\}\,.
\end{aligned}$$

Next, we proceed exactly as in [11, 26] to derive the HDG formulation of (2.2). That is, testing the equations in (2.2) with elements in the foregoing subspaces, integrating on each $T\in\mathcal{T}_h$ by parts, and introducing the numerical fluxes $\widehat{\boldsymbol{\sigma}_h\boldsymbol{n}}$ and $\widehat{\mathbf{u}}_h$, we arrive at: Find $(\boldsymbol{\sigma}_h, \mathbf{u}_h, \boldsymbol{\lambda}_h)\in\mathbb{H}_h\times\mathbf{Q}_h\times\mathbf{M}_h$, such that

$$\begin{aligned}
\frac{1}{\nu}(\boldsymbol{\sigma}_h^{\mathrm{d}},\boldsymbol{\tau}_h^{\mathrm{d}})_{\mathcal{T}_h} \,+\, (\mathbf{u}_h,\mathbf{div}_h(\boldsymbol{\tau}_h))_{\mathcal{T}_h} \,-\, \langle\boldsymbol{\tau}_h\boldsymbol{n},\widehat{\mathbf{u}}_h\rangle_{\partial\mathcal{T}_h} &= 0 && \forall\,\boldsymbol{\tau}_h\in\mathbb{H}_h\,,\\
-(\boldsymbol{\sigma}_h,\nabla_h\mathbf{v}_h)_{\mathcal{T}_h} \,+\, \langle\widehat{\boldsymbol{\sigma}_h\boldsymbol{n}},\mathbf{v}_h\rangle_{\partial\mathcal{T}_h} \,-\, \alpha\,(\mathbf{u}_h,\mathbf{v}_h)_{\mathcal{T}_h} &= -(\mathbf{f},\mathbf{v}_h)_{\mathcal{T}_h} && \forall\,\mathbf{v}_h\in\mathbf{Q}_h\,,\\
\langle\widehat{\boldsymbol{\sigma}_h\boldsymbol{n}},\boldsymbol{\mu}_h\rangle_{\partial\mathcal{T}_h\backslash\Gamma} &= 0 && \forall\,\boldsymbol{\mu}_h\in\mathbf{M}_h\,,\\
(\mathrm{tr}(\boldsymbol{\sigma}_h),1)_\Omega &= 0\,,
\end{aligned} \tag{3.1}$$

where, the broken divergence operator $\mathbf{div}_h$ is defined by $\mathbf{div}_h(\boldsymbol{\tau}_h) := \mathbf{div}(\boldsymbol{\tau}_h|_T) \quad \forall\, T \in \mathcal{T}_h, \forall\, \boldsymbol{\tau}_h \in \mathbb{H}_h$, whereas the operator ∇_h is given by $\nabla_h(\mathbf{v}_h) := \nabla(\mathbf{v}_h|_T) \quad \forall\, T \in \mathcal{T}_h, \forall\, \mathbf{v}_h \in \mathbf{Q}_h$. Furthermore, letting $\boldsymbol{P}_\Gamma$ be the $\mathbf{L}^2(\Gamma)$-projection onto the space of piecewise polynomials of degree less than or equals to k on $\mathcal{E}_h^\partial$, we set the numerical fluxes as

$$\widehat{\mathbf{u}}_h \;:=\; \begin{cases} \boldsymbol{P}_\Gamma(\mathbf{g}) & \text{on } \mathcal{E}_h^\partial\,, \\ \boldsymbol{\lambda}_h & \text{on } \mathcal{E}_h^i\,, \end{cases} \qquad \text{and} \qquad \widehat{\boldsymbol{\sigma}_h \boldsymbol{n}} \;:=\; \boldsymbol{\sigma}_h \boldsymbol{n} \,-\, \mathbf{S}(\mathbf{u}_h - \widehat{\mathbf{u}}_h) \;\text{ on }\; \partial\mathcal{T}_h\,, \tag{3.2}$$

where, as is usual, $\mathbf{S}$ is an stabilization tensor. In particular, given $F \in \mathcal{E}_h$, for now on we assume that $\mathbf{S}|_F$ is a symmetric and positive definite constant tensor.

Next, using the fact that

$$-(\boldsymbol{\sigma}_h, \nabla_h \mathbf{v}_h)_{\mathcal{T}_h} \;=\; (\mathbf{v}_h, \mathbf{div}_h(\boldsymbol{\sigma}_h))_{\mathcal{T}_h} \;-\; \langle \boldsymbol{\sigma}_h \boldsymbol{n}, \mathbf{v}_h \rangle_{\partial\mathcal{T}_h}\,,$$

and the numerical traces (3.2), our problem becomes: Find $(\boldsymbol{\sigma}_h, \mathbf{u}_h, \boldsymbol{\lambda}_h) \in \mathbb{H}_h \times \mathbf{Q}_h \times \mathbf{M}_h$ such that

$$\begin{aligned} \frac{1}{\nu}\,(\boldsymbol{\sigma}_h^{\mathrm{d}}, \boldsymbol{\tau}_h^{\mathrm{d}})_{\mathcal{T}_h} \,+\, (\mathbf{u}_h, \mathbf{div}_h(\boldsymbol{\tau}_h))_{\mathcal{T}_h} \,-\, \langle \boldsymbol{\tau}_h \boldsymbol{n}, \boldsymbol{\lambda}_h \rangle_{\partial\mathcal{T}_h \setminus \Gamma} &= \langle \boldsymbol{\tau}_h \boldsymbol{n}, \mathbf{g} \rangle_\Gamma\,, \\ (\mathbf{v}_h, \mathbf{div}_h(\boldsymbol{\sigma}_h))_{\mathcal{T}_h} \,-\, \langle \mathbf{S}(\mathbf{u}_h - \boldsymbol{\lambda}_h), \mathbf{v}_h \rangle_{\partial\mathcal{T}_h \setminus \Gamma} & \\ -\, \langle \mathbf{S}\mathbf{u}_h, \mathbf{v}_h \rangle_\Gamma \,-\, \alpha\,(\mathbf{u}_h, \mathbf{v}_h)_{\mathcal{T}_h} &= -(\mathbf{f}, \mathbf{v}_h)_{\mathcal{T}_h} \,-\, \langle \mathbf{S}\mathbf{g}, \mathbf{v}_h \rangle_\Gamma\,, \\ \langle \boldsymbol{\sigma}_h \boldsymbol{n}, \boldsymbol{\mu}_h \rangle_{\partial\mathcal{T}_h \setminus \Gamma} \,-\, \langle \mathbf{S}(\mathbf{u}_h - \boldsymbol{\lambda}_h), \boldsymbol{\mu}_h \rangle_{\partial\mathcal{T}_h \setminus \Gamma} &= 0\,, \\ (\mathrm{tr}(\boldsymbol{\sigma}_h), 1)_\Omega &= 0\,, \end{aligned} \tag{3.3}$$

for all $(\boldsymbol{\tau}_h, \mathbf{v}_h, \boldsymbol{\mu}_h) \in \mathbb{H}_h \times \mathbf{Q}_h \times \mathbf{M}_h$. Then, the following theorem establishes the unique solvability of the HDG scheme (3.3).

Theorem 3.1 (Solvability analysis)**.** *There exists a unique solution for the linear problem* (3.3)*.*

Proof. In what follows, we proceed as [28, Theorem 3.1]. Indeed, we use the fact that the existence of the solution follows from its uniqueness. Thus, it suffices to show that when the right-hand sides of (3.3) vanish, then $\boldsymbol{\sigma}_h$, $\mathbf{u}_h$, and $\boldsymbol{\lambda}_h$ also vanish. According to the above discussion, we assume that $\mathbf{f} = \mathbf{0}$ and $\mathbf{g} = \mathbf{0}$, and taking $\boldsymbol{\tau}_h := \boldsymbol{\sigma}_h$, $\mathbf{v}_h := -\mathbf{u}_h$ and $\boldsymbol{\mu}_h := \boldsymbol{\lambda}_h$ in (3.3), we can show that

$$\frac{1}{\nu}\|\boldsymbol{\sigma}_h^{\mathrm{d}}\|_{0,\Omega}^2 \;+\; \alpha\|\mathbf{u}_h\|_{0,\Omega}^2 \;+\; \langle \mathbf{S}(\mathbf{u}_h - \boldsymbol{\lambda}_h), \mathbf{u}_h - \boldsymbol{\lambda}_h \rangle_{\partial\mathcal{T}_h \setminus \Gamma} \;+\; \langle \mathbf{S}\mathbf{u}_h, \mathbf{u}_h \rangle_\Gamma \;=\; 0\,,$$

which, using the properties of ν, α and $\mathbf{S}$, it follows that

$$\boldsymbol{\sigma}_h^{\mathrm{d}} \,=\, \mathbf{0} \quad \text{in} \quad \Omega\,, \qquad \mathbf{u}_h \,=\, \mathbf{0} \quad \text{in} \quad \Omega\,, \quad \text{and} \quad \mathbf{u}_h \,=\, \boldsymbol{\lambda}_h \quad \text{on} \quad \mathcal{E}_h^i\,. \tag{3.4}$$

Now, using the last two identities of (3.4) we obtain that $\boldsymbol{\lambda}_h = \mathbf{0}$ on $\mathcal{E}_h^i$. Thus, from the second and third equations of (3.3), we deduce that $\mathbf{div}_h(\boldsymbol{\sigma}_h) = \mathbf{0}$ in Ω and $[\![\boldsymbol{\sigma}_h \boldsymbol{n}]\!] = \mathbf{0}$ on $\mathcal{E}_h^i$, respectively, which together with $\boldsymbol{\sigma}_h^{\mathrm{d}} = \mathbf{0}$ in Ω implies that $\boldsymbol{\sigma}_h = c\,\mathbb{I}$ in Ω, where $c \in \mathrm{R}$. Finally, applying that $(\mathrm{tr}(\boldsymbol{\sigma}_h), 1)_\Omega = 0$, we arrive to $\boldsymbol{\sigma}_h = \mathbf{0}$ in Ω and completes the proof. □

3.1 A priori error analysis

In this section we aim to derive the *a priori* error estimates for the HDG scheme (3.3) and the continuous formulation (2.4). In order to do that, in the next result we establish the converse of the derivation of (2.4).

Lemma 3.1. *Let* $(\boldsymbol{\sigma},\mathbf{u})\in\mathbb{H}\times\mathbf{Q}$ *be the unique solution of* (2.4)*. Then,* $\nabla\mathbf{u}=\frac{1}{\nu}\,\boldsymbol{\sigma}^{\rm d}$ *in* Ω *(which implies that* $\mathbf{u}\in\mathbf{H}^1(\Omega)$*),* $\mathbf{u}=\mathbf{g}$ *on* Γ*, and* $\alpha\,\mathbf{u}-\mathbf{div}(\boldsymbol{\sigma})=\mathbf{f}$ *in* Ω*.*

Proof. We begin by looking from the first equation of (2.4) that, in particular, yields

$$\frac{1}{\nu}\int_\Omega \boldsymbol{\sigma}^{\rm d}:\boldsymbol{\tau}\;+\;\int_\Omega \mathbf{u}\cdot\mathbf{div}(\boldsymbol{\tau})\;=\;0\qquad\forall\;\boldsymbol{\tau}\in[C_0^\infty(\Omega)]^{n\times n}\,,$$

which, establishes that $\nabla\mathbf{u}=\frac{1}{\nu}\,\boldsymbol{\sigma}^{\rm d}$ in $[\mathcal{D}'(\Omega)]^{n\times n}$, and hence $\mathbf{u}\in\mathbf{H}^1(\Omega)$. Next, going back to the first equation of (2.4) and integrating the second term by parts, we get $\langle\boldsymbol{\tau}\boldsymbol{n},\mathbf{u}-\mathbf{g}\rangle_\Gamma=0$ for all $\boldsymbol{\tau}\in\mathbb{H}$, which gives $\mathbf{u}=\mathbf{g}$ on Γ. Finally, we show that $\alpha\,\mathbf{u}-\mathbf{div}(\boldsymbol{\sigma})=\mathbf{f}$ in Ω from (2.6). □

Now, given $r\geq 0$, we define

$$H^r(\mathcal{T}_h)\;:=\;\Big\{v\in L^2(\Omega)\;:\;v|_T\in H^r(T)\quad\forall\;T\in\mathcal{T}_h\Big\}\,,$$

whence $\mathbf{H}^r(\mathcal{T}_h)$ and $\mathbb{H}^r(\mathcal{T}_h)$ denote the vectorial and tensorial versions of $H^r(\mathcal{T}_h)$, respectively. Furthermore, we recall from [28, Section IV.A] the projection operator $\Pi_h:\mathbb{H}^1(\mathcal{T}_h)\times\mathbf{H}^1(\mathcal{T}_h)\to\mathbb{H}_h\times\mathbf{Q}_h$ which, given $(\boldsymbol{\rho},\mathbf{w})\in\mathbb{H}^1(\mathcal{T}_h)\times\mathbf{H}^1(\mathcal{T}_h)$, the values of $\Pi_h(\boldsymbol{\rho},\mathbf{w}):=(\Pi\boldsymbol{\rho},\Pi\mathbf{w})\in\mathbb{H}_h\times\mathbf{Q}_h$ on any $T\in\mathcal{T}_h$ are characterized by the following identities:

$$\begin{aligned}(\Pi\boldsymbol{\rho},\boldsymbol{\tau})_T&=(\boldsymbol{\rho},\boldsymbol{\tau})_T\qquad\forall\;\boldsymbol{\tau}\in\mathbb{P}_{k-1}(T)\,,\\ (\Pi\mathbf{w},\mathbf{v})_T&=(\mathbf{w},\mathbf{v})_T\qquad\forall\;\mathbf{v}\in\mathbf{P}_{k-1}(T)\,,\\ \langle\Pi\boldsymbol{\rho}\boldsymbol{n}-\mathbf{S}\Pi\mathbf{w},\boldsymbol{\mu}\rangle_F&=\langle\boldsymbol{\rho}\boldsymbol{n}-\mathbf{S}\mathbf{w},\boldsymbol{\mu}\rangle_F\qquad\forall\;\boldsymbol{\mu}\in\mathbf{P}_k(F)\,,\quad\forall\;F\in\partial T\,,\end{aligned}\tag{3.5}$$

which, satisfies the approximation properties (see [28, Theorem 4.1]):

$$\|\Pi\mathbf{w}-\mathbf{w}\|_{0,T}\;\leq\;C\Big\{h_T^{\ell_{\mathbf{w}}+1}|\mathbf{w}|_{\ell_{\mathbf{w}}+1,T}\;+\;h_T^{\ell_{\boldsymbol{\rho}}+1}|\mathbf{div}(\boldsymbol{\rho})|_{\ell_{\boldsymbol{\rho}},T}\Big\}\,,\tag{3.6}$$

and

$$\|\Pi\boldsymbol{\rho}-\boldsymbol{\rho}\|_{0,T}\;\leq\;C\Big\{h_T^{\ell_{\boldsymbol{\rho}}+1}|\boldsymbol{\rho}|_{\ell_{\boldsymbol{\rho}}+1,T}\;+\;h_T^{\ell_{\mathbf{w}}+1}|\mathbf{w}|_{\ell_{\mathbf{w}}+1,T}\;+\;h_T^{\ell_{\boldsymbol{\rho}}+1}|\mathbf{div}(\boldsymbol{\rho})|_{\ell_{\boldsymbol{\rho}},T}\Big\}\,,\tag{3.7}$$

for $\ell_{\boldsymbol{\rho}},\ell_{\mathbf{w}}\in[0,k]$. In what follows we assume that the solution $(\boldsymbol{\sigma},\mathbf{u})$ of our problem (2.4) is regular enough to apply Π_h.

On the other hand, using Lemma 3.1 and the consistency in the numerical fluxes (cf. (3.2)) of the HDG approximation, we note that the exact solution $(\boldsymbol{\sigma},\,\mathbf{u},\,\boldsymbol{\lambda}:=\mathbf{u}|_{\mathcal{E}_h^i})$, satisfies also (3.3). Hence, after applying the definition of the projection Π_h (cf. (3.5)), integrating by parts, and performing simple algebraic manipulations, we find the error equations:

$$\frac{1}{\nu}\,((\mathrm{E}^{\boldsymbol{\sigma}})^{\rm d},\boldsymbol{\tau}_h^{\rm d})_{\mathcal{T}_h}\;+\;(\mathrm{E}^{\mathbf{u}},\mathbf{div}_h(\boldsymbol{\tau}_h))_{\mathcal{T}_h}\;-\;\langle\boldsymbol{\tau}_h\boldsymbol{n},\mathrm{E}^{\boldsymbol{\lambda}}\rangle_{\partial\mathcal{T}_h\setminus\Gamma}\;=\;\frac{1}{\nu}\,(\Pi\boldsymbol{\sigma}-\boldsymbol{\sigma},\boldsymbol{\tau}_h^{\rm d})_{\mathcal{T}_h}\,,\tag{3.8a}$$

$$\begin{aligned}(\mathbf{v}_h,\mathbf{div}_h(\mathrm{E}^{\boldsymbol{\sigma}}))_{\mathcal{T}_h}\;-\;\langle\mathbf{S}(\mathrm{E}^{\mathbf{u}}-\mathrm{E}^{\boldsymbol{\lambda}}),\mathbf{v}_h\rangle_{\partial\mathcal{T}_h\setminus\Gamma}&\\ -\;\langle\mathbf{S}\mathrm{E}^{\mathbf{u}},\mathbf{v}_h\rangle_\Gamma\;-\;\alpha\,(\mathrm{E}^{\mathbf{u}},\mathbf{v}_h)_{\mathcal{T}_h}&=-\alpha\,(\Pi\mathbf{u}-\mathbf{u},\mathbf{v}_h)_{\mathcal{T}_h}\,,\end{aligned}\tag{3.8b}$$

$$\langle\mathrm{E}^{\boldsymbol{\sigma}}\boldsymbol{n},\boldsymbol{\mu}_h\rangle_{\partial\mathcal{T}_h\setminus\Gamma}\;-\;\langle\mathbf{S}(\mathrm{E}^{\mathbf{u}}-\mathrm{E}^{\boldsymbol{\lambda}}),\boldsymbol{\mu}_h\rangle_{\partial\mathcal{T}_h\setminus\Gamma}\;=\;0\,,\tag{3.8c}$$

$$(\mathrm{tr}(\mathrm{E}^{\boldsymbol{\sigma}}),1)_\Omega\;=\;(\mathrm{tr}(\Pi\boldsymbol{\sigma}-\boldsymbol{\sigma}),1)_\Omega\,,\tag{3.8d}$$

for all $(\boldsymbol{\tau}_h,\mathbf{v}_h,\boldsymbol{\mu}_h)\in\mathbb{H}_h\times\mathbf{Q}_h\times\mathbf{M}_h$, where $\mathrm{E}^{\boldsymbol{\sigma}}:=\Pi\boldsymbol{\sigma}-\boldsymbol{\sigma}_h$, $\mathrm{E}^{\mathbf{u}}:=\Pi\mathbf{u}-\mathbf{u}_h$ and $\mathrm{E}^{\boldsymbol{\lambda}}:=\boldsymbol{P}_M(\mathbf{u})-\boldsymbol{\lambda}_h$, are the approximation errors, with $\boldsymbol{P}_M:\mathbf{L}^2(\mathcal{E}_h^i)\to\mathbf{M}_h$ the $\mathbf{L}^2(\mathcal{E}_h^i)$-orthogonal projection.

Our next goal is to provide upper estimates for the approximation errors. Thus, we begin by determining estimates for $\|\mathrm{E}^{\mathbf{u}}\|_{0,\Omega}$ and $\|\mathrm{E}^{\boldsymbol{\sigma}}\|_{0,\Omega}$ in the following two lemmas.

Lemma 3.2. *There exists $C > 0$, independent of h, such that*

$$\|(\mathrm{E}^{\boldsymbol{\sigma}})^{\mathrm{d}}\|_{0,\Omega} \;+\; \|\mathrm{E}^{\mathbf{u}}\|_{0,\Omega} \;+\; \langle \mathbf{S}(\mathrm{E}^{\mathbf{u}} - \mathrm{E}^{\boldsymbol{\lambda}}), \mathrm{E}^{\mathbf{u}} - \mathrm{E}^{\boldsymbol{\lambda}} \rangle^{1/2}_{\partial\mathcal{T}_h\setminus\Gamma} \;+\; \langle \mathbf{S}\mathrm{E}^{\mathbf{u}}, \mathrm{E}^{\mathbf{u}} \rangle^{1/2}_{\Gamma} \\ \leq\; C \left\{ \|\Pi\boldsymbol{\sigma} - \boldsymbol{\sigma}\|_{0,\Omega} \;+\; \|\Pi\mathbf{u} - \mathbf{u}\|_{0,\Omega} \right\}.$$

Proof. First, we add the error equations (3.8a)-(3.8b)-(3.8c), with $\boldsymbol{\tau}_h := \mathrm{E}^{\boldsymbol{\sigma}}$, $\mathbf{v}_h := -\mathrm{E}^{\mathbf{u}}$ and $\boldsymbol{\mu}_h := \mathrm{E}^{\boldsymbol{\lambda}}$, to find that

$$\frac{1}{\nu}\,\|(\mathrm{E}^{\boldsymbol{\sigma}})^{\mathrm{d}}\|^2_{0,\Omega} \;+\; \alpha\,\|\mathrm{E}^{\mathbf{u}}\|^2_{0,\Omega} \;+\; \langle \mathbf{S}(\mathrm{E}^{\mathbf{u}} - \mathrm{E}^{\boldsymbol{\lambda}}), \mathrm{E}^{\mathbf{u}} - \mathrm{E}^{\boldsymbol{\lambda}} \rangle_{\partial\mathcal{T}_h\setminus\Gamma} \;+\; \langle \mathbf{S}\mathrm{E}^{\mathbf{u}}, \mathrm{E}^{\mathbf{u}} \rangle_{\Gamma} \\ =\; \frac{1}{\nu}\,(\Pi\boldsymbol{\sigma} - \boldsymbol{\sigma}, (\mathrm{E}^{\boldsymbol{\sigma}})^{\mathrm{d}})_{\mathcal{T}_h} \;+\; \alpha\,(\Pi\mathbf{u} - \mathbf{u}, \mathrm{E}^{\mathbf{u}})_{\mathcal{T}_h}\,.$$

The result now follows by using the Cauchy-Schwarz and Young inequalities in the right-hand side of the previous identity. □

Lemma 3.3. *There exists $C > 0$, independent of h, such that*

$$\|\mathrm{E}^{\boldsymbol{\sigma}}\|_{0,\Omega} \;\leq\; C \left\{ \|\Pi\boldsymbol{\sigma} - \boldsymbol{\sigma}\|_{0,\Omega} \;+\; \|\Pi\mathbf{u} - \mathbf{u}\|_{0,\Omega} \right\}.$$

Proof. We adapt the proofs of [11, Proposition 3.4] and [28, Lemma 4.5]. Indeed, from the identity $\|\mathrm{E}^{\boldsymbol{\sigma}}\|^2_{0,\Omega} = \|(\mathrm{E}^{\boldsymbol{\sigma}})^{\mathrm{d}}\|^2_{0,\Omega} + \frac{1}{n}\,\|\mathrm{tr}(\mathrm{E}^{\boldsymbol{\sigma}})\|^2_{0,\Omega}$ and Lemma 3.2, it is easy to see that we only need an upper estimate for $\|\mathrm{tr}(\mathrm{E}^{\boldsymbol{\sigma}})\|_{0,\Omega}$. Thus, using the fact that $\mathrm{tr}(\mathrm{E}^{\boldsymbol{\sigma}}) - \frac{1}{|\Omega|}(\mathrm{tr}(\mathrm{E}^{\boldsymbol{\sigma}}), 1)_{\Omega} \in L^2_0(\Omega)$, and a well-known continuous inf-sup condition (see, e.g. [29, Corollary 2.4 in Chapter I]), we establish that there exists $\beta > 0$ such that

$$\beta \left\| \mathrm{tr}(\mathrm{E}^{\boldsymbol{\sigma}}) - \frac{1}{|\Omega|}(\mathrm{tr}(\mathrm{E}^{\boldsymbol{\sigma}}), 1)_{\Omega} \right\|_{0,\Omega} \;\leq\; \sup_{\substack{\mathbf{v}\in\mathbf{H}^1_0(\Omega)\\ \mathbf{v}\neq\mathbf{0}}} \frac{(\mathrm{tr}(\mathrm{E}^{\boldsymbol{\sigma}}), \mathrm{div}(\mathbf{v}))_{\mathcal{T}_h}}{\|\mathbf{v}\|_{1,\Omega}}\,,$$

which, along with (3.8d), yield

$$\|\mathrm{tr}(\mathrm{E}^{\boldsymbol{\sigma}})\|_{0,\Omega} \;\leq\; \frac{1}{\beta} \sup_{\substack{\mathbf{v}\in\mathbf{H}^1_0(\Omega)\\ \mathbf{v}\neq\mathbf{0}}} \frac{(\mathrm{tr}(\mathrm{E}^{\boldsymbol{\sigma}}), \mathrm{div}(\mathbf{v}))_{\mathcal{T}_h}}{\|\mathbf{v}\|_{1,\Omega}} \;+\; n^{1/2}\|\Pi\boldsymbol{\sigma} - \boldsymbol{\sigma}\|_{0,\Omega}\,. \tag{3.9}$$

Now, letting $\mathcal{P}^k_h : \mathbf{L}^2(\Omega) \to \mathbf{Q}_h$ be the $\mathbf{L}^2(\Omega)$-orthogonal projector, it follows integrating by parts on each $T \in \mathcal{T}_h$, using the fact that $\frac{1}{n}\mathrm{tr}(\mathrm{E}^{\boldsymbol{\sigma}})\mathbb{I} = \mathrm{E}^{\boldsymbol{\sigma}} - (\mathrm{E}^{\boldsymbol{\sigma}})^{\mathrm{d}}$, and at the end incorporating the projectors $\boldsymbol{P}_M$ and $\mathcal{P}^k_h$, that for all $\mathbf{v} \in \mathbf{H}^1_0(\Omega)$ there hold

$$\begin{aligned}
\frac{1}{n}\,(\mathrm{tr}(\mathrm{E}^{\boldsymbol{\sigma}}), \mathrm{div}(\mathbf{v}))_{\mathcal{T}_h} \;&=\; -\frac{1}{n}\,(\nabla_h \mathrm{tr}(\mathrm{E}^{\boldsymbol{\sigma}}), \mathbf{v})_{\mathcal{T}_h} \;+\; \frac{1}{n}\,\langle \mathbf{v}\cdot\boldsymbol{n}, \mathrm{tr}(\mathrm{E}^{\boldsymbol{\sigma}})\rangle_{\partial\mathcal{T}_h\setminus\Gamma} \\
&=\; -\frac{1}{n}\,(\mathbf{div}_h(\mathrm{tr}(\mathrm{E}^{\boldsymbol{\sigma}})\,\mathbb{I}), \mathbf{v})_{\mathcal{T}_h} \;+\; \frac{1}{n}\,\langle (\mathrm{tr}(\mathrm{E}^{\boldsymbol{\sigma}})\,\mathbb{I})\boldsymbol{n}, \mathbf{v}\rangle_{\partial\mathcal{T}_h\setminus\Gamma} \\
&=\; (\mathbf{div}_h\big((\mathrm{E}^{\boldsymbol{\sigma}})^{\mathrm{d}}\big), \mathbf{v})_{\mathcal{T}_h} \;-\; (\mathbf{div}_h(\mathrm{E}^{\boldsymbol{\sigma}}), \mathbf{v})_{\mathcal{T}_h} \;+\; \langle \mathrm{E}^{\boldsymbol{\sigma}}\boldsymbol{n}, \mathbf{v}\rangle_{\partial\mathcal{T}_h\setminus\Gamma} \;-\; \langle (\mathrm{E}^{\boldsymbol{\sigma}})^{\mathrm{d}}\boldsymbol{n}, \mathbf{v}\rangle_{\partial\mathcal{T}_h\setminus\Gamma} \\
&=\; -((\mathrm{E}^{\boldsymbol{\sigma}})^{\mathrm{d}}, \nabla\mathbf{v})_{\mathcal{T}_h} \;-\; (\mathcal{P}^k_h(\mathbf{v}), \mathbf{div}_h(\mathrm{E}^{\boldsymbol{\sigma}}))_{\mathcal{T}_h} \;+\; \langle \mathrm{E}^{\boldsymbol{\sigma}}\boldsymbol{n}, \boldsymbol{P}_M(\mathbf{v})\rangle_{\partial\mathcal{T}_h\setminus\Gamma}\,.
\end{aligned}$$

Next, employing the error equations (3.8b) and (3.8c) with $\mathbf{v}_h := \mathcal{P}_h^k(\mathbf{v})$ and $\boldsymbol{\mu}_h := \boldsymbol{P}_M(\mathbf{v})$, respectively, we deduce together with the foregoing equation that

$$
\begin{aligned}
\frac{1}{n}\,(\mathrm{tr}(\mathrm{E}^{\boldsymbol{\sigma}}),\mathrm{div}(\mathbf{v}))_{\mathcal{T}_h} \;&=\; -((\mathrm{E}^{\boldsymbol{\sigma}})^{\mathrm{d}},\nabla\mathbf{v})_{\mathcal{T}_h} \;-\; \langle \mathbf{S}(\mathrm{E}^{\mathbf{u}}-\mathrm{E}^{\boldsymbol{\lambda}}),\mathcal{P}_h^k(\mathbf{v})-\boldsymbol{P}_M(\mathbf{v})\rangle_{\partial\mathcal{T}_h\setminus\Gamma}\\
&\quad -\; \langle \mathbf{S}\mathrm{E}^{\mathbf{u}},\mathcal{P}_h^k(\mathbf{v})\rangle_{\Gamma} \;-\; \alpha\,(\mathrm{E}^{\mathbf{u}},\mathcal{P}_h^k(\mathbf{v}))_{\mathcal{T}_h} \;+\; \alpha\,(\Pi\mathbf{u}-\mathbf{u},\mathcal{P}_h^k(\mathbf{v}))_{\mathcal{T}_h}\\
&=\; -((\mathrm{E}^{\boldsymbol{\sigma}})^{\mathrm{d}},\nabla\mathbf{v})_{\mathcal{T}_h} \;-\; \langle \mathbf{S}(\mathrm{E}^{\mathbf{u}}-\mathrm{E}^{\boldsymbol{\lambda}}),\mathcal{P}_h^k(\mathbf{v})-\boldsymbol{P}_M(\mathbf{v})\rangle_{\partial\mathcal{T}_h\setminus\Gamma} \;-\; \langle \mathbf{S}\mathrm{E}^{\mathbf{u}},\mathcal{P}_h^k(\mathbf{v})\rangle_{\Gamma}\\
&\quad -\; \alpha\,(\mathrm{E}^{\mathbf{u}},\mathbf{v})_{\mathcal{T}_h} \;+\; \alpha\,(\Pi\mathbf{u}-\mathbf{u},\mathcal{P}_h^k(\mathbf{v}))_{\mathcal{T}_h}\\
&\leq\; \|(\mathrm{E}^{\boldsymbol{\sigma}})^{\mathrm{d}}\|_{0,\Omega}|\mathbf{v}|_{1,\Omega} \;+\; \langle \mathbf{S}(\mathrm{E}^{\mathbf{u}}-\mathrm{E}^{\boldsymbol{\lambda}}),\mathrm{E}^{\mathbf{u}}-\mathrm{E}^{\boldsymbol{\lambda}}\rangle_{\partial\mathcal{T}_h\setminus\Gamma}^{1/2}\,\langle \mathbf{S}\big(\mathcal{P}_h^k(\mathbf{v})-\boldsymbol{P}_M(\mathbf{v})\big),\mathcal{P}_h^k(\mathbf{v})-\boldsymbol{P}_M(\mathbf{v})\rangle_{\partial\mathcal{T}_h\setminus\Gamma}^{1/2}\\
&\quad +\; \langle \mathbf{S}\mathrm{E}^{\mathbf{u}},\mathrm{E}^{\mathbf{u}}\rangle_{\Gamma}^{1/2}\,\langle \mathbf{S}\mathcal{P}_h^k(\mathbf{v}),\mathcal{P}_h^k(\mathbf{v})\rangle_{\Gamma}^{1/2} \;+\; \alpha\|\mathrm{E}^{\mathbf{u}}\|_{0,\Omega}\|\mathbf{v}\|_{0,\Omega} \;+\; \alpha\|\Pi\mathbf{u}-\mathbf{u}\|_{0,\Omega}\|\mathcal{P}_h^k(\mathbf{v})\|_{0,\Omega}\\
&\leq\; \Bigg\{\|(\mathrm{E}^{\boldsymbol{\sigma}})^{\mathrm{d}}\|_{0,\Omega} \;+\; \langle \mathbf{S}(\mathrm{E}^{\mathbf{u}}-\mathrm{E}^{\boldsymbol{\lambda}}),\mathrm{E}^{\mathbf{u}}-\mathrm{E}^{\boldsymbol{\lambda}}\rangle_{\partial\mathcal{T}_h\setminus\Gamma}^{1/2}\,\frac{\langle \mathbf{S}\big(\mathcal{P}_h^k(\mathbf{v})-\boldsymbol{P}_M(\mathbf{v})\big),\mathcal{P}_h^k(\mathbf{v})-\boldsymbol{P}_M(\mathbf{v})\rangle_{\partial\mathcal{T}_h\setminus\Gamma}^{1/2}}{\|\mathbf{v}\|_{1,\Omega}}\\
&\quad +\; \langle \mathbf{S}\mathrm{E}^{\mathbf{u}},\mathrm{E}^{\mathbf{u}}\rangle_{\Gamma}^{1/2}\,\frac{\langle \mathbf{S}\mathcal{P}_h^k(\mathbf{v}),\mathcal{P}_h^k(\mathbf{v})\rangle_{\Gamma}^{1/2}}{\|\mathbf{v}\|_{1,\Omega}} \;+\; \alpha\|\mathrm{E}^{\mathbf{u}}\|_{0,\Omega} \;+\; \alpha\|\Pi\mathbf{u}-\mathbf{u}\|_{0,\Omega}\Bigg\}\|\mathbf{v}\|_{1,\Omega}\quad\forall\;\mathbf{v}\in\mathbf{H}_0^1(\Omega)\,,
\end{aligned}
$$

where, in the last inequality, we applied the fact that $\|\mathcal{P}_h^k(\mathbf{v})\|_{0,\Omega}\leq\|\mathbf{v}\|_{0,\Omega}$. Then, replacing back the above identity into (3.9), yields

$$
\begin{aligned}
\|\mathrm{tr}(\mathrm{E}^{\boldsymbol{\sigma}})\|_{0,\Omega} \;&\leq\; \frac{n}{\beta}\,(1+\alpha)\Big\{\|(\mathrm{E}^{\boldsymbol{\sigma}})^{\mathrm{d}}\|_{0,\Omega} \;+\; \|\mathrm{E}^{\mathbf{u}}\|_{0,\Omega} \;+\; \|\Pi\mathbf{u}-\mathbf{u}\|_{0,\Omega}\Big\}\\
&\quad +\; \frac{n\sqrt{2}}{\beta}\,\Psi(\mathbf{S})\,\Big\{\langle \mathbf{S}(\mathrm{E}^{\mathbf{u}}-\mathrm{E}^{\boldsymbol{\lambda}}),\mathrm{E}^{\mathbf{u}}-\mathrm{E}^{\boldsymbol{\lambda}}\rangle_{\partial\mathcal{T}_h\setminus\Gamma}^{1/2} \;+\; \langle \mathbf{S}\mathrm{E}^{\mathbf{u}},\mathrm{E}^{\mathbf{u}}\rangle_{\Gamma}^{1/2}\Big\}\\
&\quad +\; n^{1/2}\,\|\Pi\boldsymbol{\sigma}-\boldsymbol{\sigma}\|_{0,\Omega}\,,
\end{aligned}
\tag{3.10}
$$

with

$$
\Psi(\mathbf{S}) \;:=\; \sup_{\substack{\mathbf{v}\in\mathbf{H}_0^1(\Omega)\\ \mathbf{v}\neq\mathbf{0}}}\;\frac{\Big\{\langle \mathbf{S}\big(\mathcal{P}_h^k(\mathbf{v})-\boldsymbol{P}_M(\mathbf{v})\big),\mathcal{P}_h^k(\mathbf{v})-\boldsymbol{P}_M(\mathbf{v})\rangle_{\partial\mathcal{T}_h\setminus\Gamma} \;+\; \langle \mathbf{S}\mathcal{P}_h^k(\mathbf{v}),\mathcal{P}_h^k(\mathbf{v})\rangle_{\Gamma}\Big\}^{1/2}}{\|\mathbf{v}\|_{1,\Omega}}\,.
$$

On the other hand, letting $\boldsymbol{P}_F^k : \mathbf{L}^2(F)\to\mathbf{P}_k(F)$ be the $\mathbf{L}^2(F)$-orthogonal projector on each $F\in\mathcal{E}_h$, we know that $\boldsymbol{P}_M(\mathbf{v})|_F=\boldsymbol{P}_F^k(\mathbf{v})\;\;\forall\;F\in\mathcal{E}_h^i$ and $\boldsymbol{P}_F^k(\mathbf{v})=\mathbf{0}\;\;\forall\;F\in\mathcal{E}_h^\partial$, for each $\mathbf{v}\in\mathbf{H}_0^1(\Omega)$. Hence, we can write

$$
\Psi(\mathbf{S}) \;=\; \sup_{\substack{\mathbf{v}\in\mathbf{H}_0^1(\Omega)\\ \mathbf{v}\neq\mathbf{0}}}\;\frac{\Big\{\sum_{T\in\mathcal{T}_h}\sum_{F\in\partial T}\langle \mathbf{S}\big(\mathcal{P}_h^k(\mathbf{v})-\boldsymbol{P}_F^k(\mathbf{v})\big),\mathcal{P}_h^k(\mathbf{v})-\boldsymbol{P}_F^k(\mathbf{v})\rangle_F\Big\}^{1/2}}{\|\mathbf{v}\|_{1,\Omega}}\,,
$$

and using the same arguments in the first part of the proof of [11, Proposition 3.9], it easy to see that $\Psi(\mathbf{S})$ is bounded by a constant depending on $\mathbf{S}$. Finally, according to the above discussion, along with Lemma 3.2, we complete the proof from (3.10). □

It is important to remark here that no duality argument was required in order to get an estimate for $\|\mathrm{E}^{\mathbf{u}}\|_{0,\Omega}$, which is the main technique used in [11, 12, 15, 28]. However, it is because of this that we can not show a superconvergence behaviour in the approximation of the trace variable $\boldsymbol{\lambda}_h$, and then we deduce an *a priori* error estimate for this variable, in similar way to [26, Theorem 4.2].

Lemma 3.4. *There exists $C > 0$, independent of h, such that*

$$\left\{ \sum_{F\in\mathcal{E}_h^i} h_F \|\mathrm{E}^{\boldsymbol{\lambda}}\|_{0,F}^2 \right\}^{1/2} \;\leq\; C \left\{ \|\mathrm{E}^{\boldsymbol{\sigma}}\|_{0,\Omega} \;+\; \|\mathrm{E}^{\mathbf{u}}\|_{0,\Omega} \right\}.$$

Proof. Notices that the error equation (3.8c) can be written as

$$\int_{\mathcal{E}_h^i} \Big\{ [\![\mathrm{E}^{\boldsymbol{\sigma}} \boldsymbol{n}]\!] - 2\,\mathbf{S}\big(\{\!\{ \mathrm{E}^{\mathbf{u}} \}\!\} - \mathrm{E}^{\boldsymbol{\lambda}} \big) \Big\} \cdot \boldsymbol{\mu}_h \;=\; 0 \qquad \forall\; \boldsymbol{\mu}_h \in \mathbf{M}_h \,,$$

where, $\{\!\{\cdot\}\!\}$ stands for the usual mean function on $\mathcal{E}_h^i$. Hence, using that $[\![\mathrm{E}^{\boldsymbol{\sigma}} \boldsymbol{n}]\!] - 2\,\mathbf{S}(\{\!\{ \mathrm{E}^{\mathbf{u}} \}\!\} - \mathrm{E}^{\boldsymbol{\lambda}}) \in \mathbf{M}_h$ and the properties of $\mathbf{S}$, we find that

$$\mathrm{E}^{\boldsymbol{\lambda}} \;=\; \{\!\{ \mathrm{E}^{\mathbf{u}} \}\!\} \;-\; \frac{1}{2}\,\mathbf{S}^{-1} [\![\mathrm{E}^{\boldsymbol{\sigma}} \boldsymbol{n}]\!] \quad \text{on} \;\; \mathcal{E}_h^i \,.$$

Now, from the above identity, it follows

$$\begin{aligned}
\sum_{F\in\mathcal{E}_h^i} h_F \|\mathrm{E}^{\boldsymbol{\lambda}}\|_{0,F}^2 \;&=\; \sum_{F\in\mathcal{E}_h^i} h_F \left\| \{\!\{ \mathrm{E}^{\mathbf{u}} \}\!\} \;-\; \frac{1}{2}\,\mathbf{S}^{-1} [\![\mathrm{E}^{\boldsymbol{\sigma}} \boldsymbol{n}]\!] \right\|_{0,F}^2 \\
&\leq\; \frac{1}{2} \sum_{F\in\mathcal{E}_h^i} h_F \Big\{ \|(\mathrm{E}^{\mathbf{u}})^+ - \mathbf{S}^{-1}(\mathrm{E}^{\boldsymbol{\sigma}})^+ \boldsymbol{n}^+ \|_{0,F}^2 \;+\; \|(\mathrm{E}^{\mathbf{u}})^- - \mathbf{S}^{-1}(\mathrm{E}^{\boldsymbol{\sigma}})^- \boldsymbol{n}^- \|_{0,F}^2 \Big\} \\
&\leq\; C \sum_{T\in\mathcal{T}_h} h_T \Big\{ \|\mathrm{E}^{\mathbf{u}}\|_{0,\partial T}^2 \;+\; \|\mathrm{E}^{\boldsymbol{\sigma}}\|_{0,\partial T}^2 \Big\},
\end{aligned}$$

where, C depends on $\mathbf{S}$ and the regularity of $\mathcal{T}_h$. Finally, applying a discrete-trace theorem and an inverse inequality, we complete the proof. □

As a consequence of the previous lemmas, now we are able to establish the *a priori* error estimates for the HDG scheme (3.3).

Theorem 3.2. *Let $(\boldsymbol{\sigma}, \mathbf{u}) \in \mathbb{H} \times \mathbf{Q}$ and $(\boldsymbol{\sigma}_h, \mathbf{u}_h) \in \mathbb{H}_h \times \mathbf{Q}_h$ be the unique solutions of* (2.4) *and* (3.3)*, respectively. In addition, let $\widehat{\mathbf{u}}_h$ be the numerical flux introduced in* (3.2)*. Then, there exists $C > 0$, independent of h, such that*

$$\|\boldsymbol{\sigma} - \boldsymbol{\sigma}_h\|_{0,\Omega} \;+\; \|\mathbf{u} - \mathbf{u}_h\|_{0,\Omega} \;\leq\; C \Big\{ \|\Pi\boldsymbol{\sigma} - \boldsymbol{\sigma}\|_{0,\Omega} \;+\; \|\Pi\mathbf{u} - \mathbf{u}\|_{0,\Omega} \Big\},$$

and

$$\left\{ \sum_{F\in\mathcal{E}_h} h_F \|\mathbf{u} - \widehat{\mathbf{u}}_h\|_{0,F}^2 \right\}^{1/2} \;\leq\; C \Big\{ \|\Pi\boldsymbol{\sigma} - \boldsymbol{\sigma}\|_{0,\Omega} \;+\; \|\Pi\mathbf{u} - \mathbf{u}\|_{0,\Omega} \Big\} \;+\; C \left\{ \sum_{F\in\mathcal{E}_h} h_F \|\boldsymbol{P}_F^k(\mathbf{u}) - \mathbf{u}\|_{0,F}^2 \right\}^{1/2}.$$

Proof. The first estimate follows straightforwardly from the triangle inequality and Lemmas 3.2 and 3.3. On the other hand, using the definitions of $\widehat{\mathbf{u}}_h$ (cf. (3.2)), $\boldsymbol{P}_M$, $\boldsymbol{P}_\Gamma$ and $\boldsymbol{P}_F^k$, along with the fact that $\mathbf{u} = \mathbf{g}$ on Γ (cf. Lemma 3.1), we find that

$$\sum_{F\in\mathcal{E}_h} h_F \|\mathbf{u} - \widehat{\mathbf{u}}_h\|_{0,F}^2 \;\leq\; 2 \sum_{F\in\mathcal{E}_h^i} h_F \|\mathrm{E}^{\boldsymbol{\lambda}}\|_{0,F}^2 \;+\; 2 \sum_{F\in\mathcal{E}_h} h_F \|\boldsymbol{P}_F^k(\mathbf{u}) - \mathbf{u}\|_{0,F}^2 \,.$$

Then, applying Lemma 3.4 into the above estimate, we complete the proof of the lemma. □

Moreover, the following theorem provides the corresponding theoretical rates of convergence.

Theorem 3.3. *Let* $(\boldsymbol{\sigma},\mathbf{u})\in\mathbb{H}\times\mathbf{Q}$ *and* $(\boldsymbol{\sigma}_h,\mathbf{u}_h)\in\mathbb{H}_h\times\mathbf{Q}_h$ *be the unique solutions of* (2.4) *and* (3.3)*, respectively. In addition, let* $\widehat{\mathbf{u}}_h$ *be the numerical flux introduced in* (3.2)*. Then, there exists* $C>0$*, independent of* h*, such that*

$$\|\boldsymbol{\sigma}-\boldsymbol{\sigma}_h\|_{0,\Omega}\ +\ \|\mathbf{u}-\mathbf{u}_h\|_{0,\Omega}\ \leq\ C\sum_{T\in\mathcal{T}_h}h_T^{\min\{\ell_{\boldsymbol{\sigma}},\ell_{\mathbf{u}}\}+1}\Big\{|\boldsymbol{\sigma}|_{\ell_{\boldsymbol{\sigma}}+1,T}\ +\ |\mathbf{div}(\boldsymbol{\sigma})|_{\ell_{\boldsymbol{\sigma}},T}\ +\ |\mathbf{u}|_{\ell_{\mathbf{u}}+1,T}\Big\},$$

and

$$\begin{aligned}\left\{\sum_{F\in\mathcal{E}_h}h_F\|\mathbf{u}-\widehat{\mathbf{u}}_h\|_{0,F}^2\right\}^{1/2}&\leq C\sum_{T\in\mathcal{T}_h}h_T^{\min\{\ell_{\boldsymbol{\sigma}},\ell_{\mathbf{u}}\}+1}\Big\{|\boldsymbol{\sigma}|_{\ell_{\boldsymbol{\sigma}}+1,T}\ +\ |\mathbf{div}(\boldsymbol{\sigma})|_{\ell_{\boldsymbol{\sigma}},T}\ +\ |\mathbf{u}|_{\ell_{\mathbf{u}}+1,T}\Big\}\\&\quad+\ C\sum_{F\in\mathcal{E}_h}h_F^{\ell_{\mathbf{u}}+1}|\mathbf{u}|_{\ell_{\mathbf{u}}+1/2,F}\,.\end{aligned}$$

for $\ell_{\boldsymbol{\sigma}},\ell_{\mathbf{u}}\in[0,k]$.

Proof. It follows from Theorem 3.2 and the approximation properties of Π_h (cf. (3.6) and (3.7)), and those of $\boldsymbol{P}_F^k$ (see, e.g. [7]). □

We end this section by recalling from (2.3) that $p=-\frac{1}{n}\mathrm{tr}(\boldsymbol{\sigma})$ in Ω, which suggests to define a postprocessed approximation of the pressure, given by

$$p_h\ :=\ -\frac{1}{n}\mathrm{tr}(\boldsymbol{\sigma}_h)\quad\text{in }\Omega\,,\tag{3.11}$$

where, from the fact that

$$\|p-p_h\|_{0,\Omega}\ \leq\ \frac{1}{n}\,\|\mathrm{tr}(\boldsymbol{\sigma}-\boldsymbol{\sigma}_h)\|_{0,\Omega}\ \leq\ \frac{1}{n^{1/2}}\,\|\boldsymbol{\sigma}-\boldsymbol{\sigma}_h\|_{0,\Omega}\,,$$

and Theorem 3.3, we obtain an *a priori error* estimate for p and p_h.

4 A posteriori error analysis

We now aim to develop a residual-based *a posteriori* error analysis for the HDG scheme (3.3). Here, we remark that the techniques from [27, Section 5] is suitably adapted. We begin by introducing additional notations. In what follows, for each $F\in\mathcal{E}_h^i$ such that $F=\overline{T}^+\cap\overline{T}^-$, we denote by $[\![\mathbf{v}\otimes\boldsymbol{n}]\!]\ :=\ \mathbf{v}^+\otimes\boldsymbol{n}^+\ +\ \mathbf{v}^-\otimes\boldsymbol{n}^-$ the jumps of vector fields on F, with $\otimes$ denotes the usual dyadic product. Similarly, for a tensor field $\boldsymbol{\tau}$, we let $[\![\boldsymbol{\tau}\times\boldsymbol{n}]\!]\ :=\ \boldsymbol{\tau}^+\times\boldsymbol{n}^+\ +\ \boldsymbol{\tau}^-\times\boldsymbol{n}^-$ be the corresponding tangential jump across F, where

$$\boldsymbol{\tau}\times\boldsymbol{n}\ :=\ \begin{pmatrix}\tau_{12}n_1-\tau_{11}n_2\\ \tau_{22}n_1-\tau_{21}n_2\end{pmatrix}\in\mathrm{R}^2\,,\quad\text{and}\quad\boldsymbol{\tau}\times\boldsymbol{n}\ :=\ \begin{pmatrix}(\tau_{11},\tau_{12},\tau_{13})\times\boldsymbol{n}\\ (\tau_{21},\tau_{22},\tau_{23})\times\boldsymbol{n}\\ (\tau_{31},\tau_{32},\tau_{33})\times\boldsymbol{n}\end{pmatrix}\in\mathrm{R}^{3\times3}\,,$$

when $n=2$ and $n=3$, respectively. Furthermore, in three space dimensions the ith row of $\mathrm{curl}(\boldsymbol{\tau})$ is nothing but $\mathrm{curl}(\cdot)$ applied to the ith row of $\boldsymbol{\tau}$. In the two-dimensional case, given vector and tensor valued fields $\mathbf{v}$ and $\boldsymbol{\tau}$, respectively, we let

$$\mathrm{curl}(\mathbf{v})\ :=\ \begin{pmatrix}\partial_{x_2}v_1 & -\partial_{x_1}v_1\\ \partial_{x_2}v_2 & -\partial_{x_1}v_2\end{pmatrix}\in\mathrm{R}^{2\times2}\quad\text{and}\quad\mathrm{curl}(\boldsymbol{\tau})\ :=\ \begin{pmatrix}\partial_{x_1}\tau_{12}-\partial_{x_2}\tau_{11}\\ \partial_{x_1}\tau_{22}-\partial_{x_2}\tau_{21}\end{pmatrix}\in\mathrm{R}^2.$$

On the other hand, we recall from [27, Section 5.1] the postprocessed flux $\boldsymbol{\sigma}_h^\star$ for the variable $\boldsymbol{\sigma}_h$ (see also [12, 13]), that is, we let $\boldsymbol{\sigma}_h^\star$ be the unique element in $\mathbb{RT}_k(\mathcal{T}_h)$ such that

$$\begin{aligned}\int_T \boldsymbol{\sigma}_h^\star : \boldsymbol{\tau}_h &= \int_T \boldsymbol{\sigma}_h : \boldsymbol{\tau}_h \quad \forall\, \boldsymbol{\tau}_h \in \mathbb{P}_{k-1}(T)\,, \quad \forall\, T \in \mathcal{T}_h\,,\\ \int_F \boldsymbol{\sigma}_h^\star \boldsymbol{n} \cdot \boldsymbol{\mu}_h &= \int_F \widehat{\boldsymbol{\sigma}_h \boldsymbol{n}} \cdot \boldsymbol{\mu}_h \quad \forall\, \boldsymbol{\mu}_h \in \mathbf{P}_k(F)\,, \quad \forall\, F \in \partial T\,, \quad \forall\, T \in \mathcal{T}_h\,,\end{aligned} \tag{4.1}$$

where $\mathbb{RT}_k(\mathcal{T}_h)$ is the global Raviart-Thomas subspace of degree k. It is important to observe here, thanks to the third equation of (3.1), that $\boldsymbol{\sigma}_h^\star \in \mathbb{H}(\mathbf{div};\Omega)$. In addition, we let $\boldsymbol{\sigma}_{h,0}^\star$ be the $\mathbb{H}_0(\mathbf{div};\Omega)$-component of $\boldsymbol{\sigma}_h^\star$, which, from the first equation of (4.1) and the fact that $(\mathrm{tr}(\boldsymbol{\sigma}_h),1)_\Omega = 0$, notice that $\boldsymbol{\sigma}_h^\star = \boldsymbol{\sigma}_{h,0}^\star$ when $k \geq 1$.

Finally, we introduce the subspace

$$X_h \,:=\, \Big\{ q \in C(\overline{\Omega}) \,:\, q|_T \in \mathrm{P}_1(T) \quad \forall\, T \in \mathcal{T}_h \Big\} \,\subset\, H^1(\Omega)\,,$$

whence $\mathbf{X}_h$ and $\mathbb{X}_h$ denote the vectorial and tensorial versions of X_h, respectively.

4.1 Reliability of the a posteriori error estimator

We begin with the following preliminary estimate.

Lemma 4.1. *Let $(\boldsymbol{\sigma},\mathbf{u}) \in \mathbb{H}\times\mathbf{Q}$ and $(\boldsymbol{\sigma}_h,\mathbf{u}_h) \in \mathbb{H}_h\times\mathbf{Q}_h$ be the unique solutions of (2.4) and (3.3), respectively. Also, let $\boldsymbol{\sigma}_h^\star \in \mathbb{H}(\mathbf{div};\Omega)$ be the postprocessed flux defined by (4.1). Then, there exists $C>0$, independent of h, such that*

$$\begin{aligned}\|\boldsymbol{\sigma}-\boldsymbol{\sigma}_h\|_{0,\Omega} \,+\, \|\mathbf{u}-\mathbf{u}_h\|_{0,\Omega} \,+\, \|\boldsymbol{\sigma}-\boldsymbol{\sigma}_{h,0}^\star\|_{\mathbf{div},\Omega} \,\leq\, C\Big\{ &\|\boldsymbol{\sigma}_h-\boldsymbol{\sigma}_{h,0}^\star\|_{0,\Omega}\\ &+\, \|\alpha\,\mathbf{u}_h - \mathbf{div}(\boldsymbol{\sigma}_{h,0}^\star)-\mathbf{f}\|_{0,\Omega} \,+\, \|\mathcal{R}\|_{\mathbb{H}'}\Big\}\,,\end{aligned} \tag{4.2}$$

where $\mathcal{R} \in \mathbb{H}'$ is defined by

$$\mathcal{R}(\boldsymbol{\tau}) \,:=\, \frac{1}{\nu}\,(\boldsymbol{\sigma}_h^{\mathrm{d}},\boldsymbol{\tau})_{\mathcal{T}_h} \,+\, (\mathbf{u}_h,\mathbf{div}(\boldsymbol{\tau}))_{\mathcal{T}_h} \,-\, \langle \boldsymbol{\tau}\boldsymbol{n},\mathbf{g}\rangle_\Gamma \qquad \forall\, \boldsymbol{\tau} \in \mathbb{H}\,. \tag{4.3}$$

In addition, when $k \geq 1$, we have that $\mathcal{R}(\boldsymbol{\tau}_h) = 0$ for all $\boldsymbol{\tau}_h \in (\mathbb{X}_h + \mathbb{RT}_0(\mathcal{T}_h)) \cap \mathbb{H}$.

Proof. Firstly, adding and subtracting $\boldsymbol{\sigma}_{h,0}^\star$, note that

$$\|\boldsymbol{\sigma}-\boldsymbol{\sigma}_h\|_{0,\Omega} + \|\mathbf{u}-\mathbf{u}_h\|_{0,\Omega} \,+\, \|\boldsymbol{\sigma}-\boldsymbol{\sigma}_{h,0}^\star\|_{\mathbf{div},\Omega} \,\leq\, \|\boldsymbol{\sigma}_h-\boldsymbol{\sigma}_{h,0}^\star\|_{0,\Omega} \,+\, 2\|(\boldsymbol{\sigma}-\boldsymbol{\sigma}_{h,0}^\star,\mathbf{u}-\mathbf{u}_h)\|_{\mathbb{H}\times\mathbf{Q}}\,. \tag{4.4}$$

Next, we take $(\boldsymbol{\rho},\mathbf{w}) := (\boldsymbol{\sigma}-\boldsymbol{\sigma}_{h,0}^\star,\mathbf{u}-\mathbf{u}_h) \in \mathbb{H}\times\mathbf{Q}$ into (2.8), in order to find that

$$\begin{aligned}C\,\|(\boldsymbol{\sigma}-\boldsymbol{\sigma}_{h,0}^\star,\mathbf{u}-\mathbf{u}_h)\|_{\mathbb{H}\times\mathbf{Q}} \,\leq\, \sup_{\substack{(\boldsymbol{\tau},\mathbf{v})\in\mathbb{H}\times\mathbf{Q}\\(\boldsymbol{\tau},\mathbf{v})\neq\mathbf{0}}} \Bigg\{ &\frac{\frac{1}{\nu}((\boldsymbol{\sigma}-\boldsymbol{\sigma}_{h,0}^\star)^{\mathrm{d}},\boldsymbol{\tau}^{\mathrm{d}})_{\mathcal{T}_h} \,+\, (\mathbf{u}-\mathbf{u}_h,\mathbf{div}(\boldsymbol{\tau}))_{\mathcal{T}_h}}{\|(\boldsymbol{\tau},\mathbf{v})\|_{\mathbb{H}\times\mathbf{Q}}}\\ &+\, \frac{(\mathbf{v},\mathbf{div}(\boldsymbol{\sigma}-\boldsymbol{\sigma}_{h,0}^\star))_{\mathcal{T}_h} \,-\, \alpha(\mathbf{u}-\mathbf{u}_h,\mathbf{v})_{\mathcal{T}_h}}{\|(\boldsymbol{\tau},\mathbf{v})\|_{\mathbb{H}\times\mathbf{Q}}}\Bigg\}\,,\end{aligned}$$

which, utilizing (2.4) and adding and subtracting $\boldsymbol{\sigma}_h$, reduces to

$$C\,\|(\boldsymbol{\sigma}-\boldsymbol{\sigma}^\star_{h,0},\mathbf{u}-\mathbf{u}_h)\|_{\mathbb{H}\times\mathbf{Q}} \;\leq\; \sup_{\substack{(\boldsymbol{\tau},\mathbf{v})\in\mathbb{H}\times\mathbf{Q}\\(\boldsymbol{\tau},\mathbf{v})\neq\mathbf{0}}}\left\{\frac{\langle\boldsymbol{\tau}\boldsymbol{n},\mathbf{g}\rangle_\Gamma \,-\, \frac{1}{\nu}(\boldsymbol{\sigma}^{\rm d}_h,\boldsymbol{\tau}^{\rm d})_{\mathcal{T}_h} \,-\, (\mathbf{u}_h,\mathbf{div}(\boldsymbol{\tau}))_{\mathcal{T}_h}}{\|(\boldsymbol{\tau},\mathbf{v})\|_{\mathbb{H}\times\mathbf{Q}}}\right.$$
$$\left. +\;\frac{\frac{1}{\nu}((\boldsymbol{\sigma}_h-\boldsymbol{\sigma}^\star_{h,0})^{\rm d},\boldsymbol{\tau}^{\rm d})_{\mathcal{T}_h} \,+\, (\alpha\,\mathbf{u}_h-\mathbf{div}(\boldsymbol{\sigma}^\star_{h,0})-\mathbf{f},\mathbf{v})_{\mathcal{T}_h}}{\|(\boldsymbol{\tau},\mathbf{v})\|_{\mathbb{H}\times\mathbf{Q}}}\right\}.$$

Then, applying the Cauchy-Schwarz inequality it follows that

$$C\,\|(\boldsymbol{\sigma}-\boldsymbol{\sigma}^\star_{h,0},\mathbf{u}-\mathbf{u}_h)\|_{\mathbb{H}\times\mathbf{Q}} \;\leq\; \frac{1}{\nu}\,\|\boldsymbol{\sigma}_h-\boldsymbol{\sigma}^\star_{h,0}\|_{0,\Omega} \;+\; \|\alpha\,\mathbf{u}_h-\mathbf{div}(\boldsymbol{\sigma}^\star_{h,0})-\mathbf{f}\|_{0,\Omega} \;+\; \|\mathcal{R}\|_{\mathbb{H}'}\,,$$

which, along with (4.4), imply (4.2). Finally, given $\boldsymbol{\tau}_h\in(\mathbb{X}_h+\mathbb{R}\mathbb{T}_0(\mathcal{T}_h))\cap\mathbb{H}$, it follows that $[\![\boldsymbol{\tau}_h\boldsymbol{n}]\!]=\mathbf{0}$ on $\mathcal{E}^i_h$ and, when $k\geq 1$, $\boldsymbol{\tau}_h\in\mathbb{H}_h$. Thus, from the first equation in (3.3), we deduce that

$$\frac{1}{\nu}\,(\boldsymbol{\sigma}^{\rm d}_h,\boldsymbol{\tau}_h)_{\mathcal{T}_h} \;+\; (\mathbf{u}_h,\mathbf{div}(\boldsymbol{\tau}_h))_{\mathcal{T}_h} \;=\; \langle\boldsymbol{\tau}_h\boldsymbol{n},\mathbf{g}\rangle_\Gamma \qquad \forall\;\boldsymbol{\tau}_h\in(\mathbb{X}_h+\mathbb{R}\mathbb{T}_0(\mathcal{T}_h))\cap\mathbb{H}\,,$$

which, completes the proof of the lemma. □

Our next goal is to bound $\|\mathcal{R}\|_{\mathbb{H}'}$ on the right-hand side of (4.2). For this end, we now introduce the Clément interpolation operator $I_h: H^1(\Omega)\to X_h$ (see [8]), which satisfies the following approximation properties: for each $v\in H^1(\Omega)$ there holds

$$\|v-I_h(v)\|_{0,T} \;\leq\; C\,h_T\,\|v\|_{1,\Delta(T)} \quad\forall\;T\in\mathcal{T}_h\,, \tag{4.5}$$

and

$$\|v-I_h(v)\|_{0,F} \;\leq\; C\,h_F^{1/2}\|v\|_{1,\Delta(F)} \quad\forall\;F\in\mathcal{E}_h\,, \tag{4.6}$$

where $\Delta(T)$ and $\Delta(F)$ are the union of all elements intersecting with T and F, respectively. In addition, we denote the vectorial and tensorial versions of I_h (both defined componentwise) by $\mathcal{I}_h:\mathbf{H}^1(\Omega)\to\mathbf{X}_h$ and $\boldsymbol{\mathcal{I}}_h:\mathbb{H}^1(\Omega)\to\mathbb{X}_h$, respectively.

Next, given $\boldsymbol{\tau}\in\mathbb{H}$ we consider its Helmholtz decomposition (see, e.g. [21, Section 4.2] for details in the two-dimensional case, and [20] in the three-dimensional case). That is, there exist $\mathbf{z}\in\mathbf{H}^2(\Omega)$ and $\boldsymbol{\varphi}\in\mathbf{H}^1(\Omega)$ such that

$$\boldsymbol{\tau} \;=\; \boldsymbol{\zeta} \;+\; \mathrm{curl}(\boldsymbol{\varphi})\,, \tag{4.7}$$

where $\boldsymbol{\zeta}:=\nabla\mathbf{z}\in\mathbb{H}^1(\Omega)$ and there holds

$$\|\boldsymbol{\zeta}\|_{1,\Omega} \;+\; \|\boldsymbol{\varphi}\|_{1,\Omega} \;\leq\; C\,\|\boldsymbol{\tau}\|_{\mathbf{div},\Omega}\,. \tag{4.8}$$

Now, we define

$$\boldsymbol{\tau}_h \;:=\; \boldsymbol{\zeta}_h \;+\; \mathrm{curl}(\boldsymbol{\varphi}_h) \;+\; c_h\mathbb{I} \;\in\; (\mathbb{X}_h+\mathbb{R}\mathbb{T}_0(\mathcal{T}_h))\cap\mathbb{H}\,,$$

where $\boldsymbol{\zeta}_h:=\boldsymbol{\mathcal{I}}_h(\boldsymbol{\zeta})$, $\boldsymbol{\varphi}_h:=\mathcal{I}_h(\boldsymbol{\varphi})$, and the constant c_h is chosen so that $(\mathrm{tr}(\boldsymbol{\tau}_h),1)_\Omega=0$. Then, for $k\geq 1$, using the definition of $\boldsymbol{\tau}_h$, the decomposition (4.7), the fact that c_h vanishes in the definition of $\mathcal{R}$ (cf. (4.3)), and Lemma 4.1, we have that

$$\mathcal{R}(\boldsymbol{\tau}) \;=\; \mathcal{R}(\boldsymbol{\tau}-\boldsymbol{\tau}_h) \;=\; \mathcal{R}_1(\boldsymbol{\zeta}) \;+\; \mathcal{R}_2(\boldsymbol{\varphi}) \qquad\forall\;\boldsymbol{\tau}\in\mathbb{H}\,, \tag{4.9}$$

where

$$\mathcal{R}_1(\boldsymbol{\zeta}) \;:=\; \mathcal{R}(\boldsymbol{\zeta}-\boldsymbol{\zeta}_h) \;=\; \frac{1}{\nu}\,(\boldsymbol{\sigma}^{\rm d}_h,\boldsymbol{\zeta}-\boldsymbol{\zeta}_h)_{\mathcal{T}_h} \;+\; (\mathbf{u}_h,\mathbf{div}(\boldsymbol{\zeta}-\boldsymbol{\zeta}_h))_{\mathcal{T}_h} \;-\; \langle(\boldsymbol{\zeta}-\boldsymbol{\zeta}_h)\boldsymbol{n},\mathbf{g}\rangle_\Gamma\,,$$

and

$$\mathcal{R}_2(\boldsymbol{\varphi}) \;:=\; \mathcal{R}(\mathrm{curl}(\boldsymbol{\varphi}-\boldsymbol{\varphi}_h)) \;=\; \frac{1}{\nu}\,(\boldsymbol{\sigma}^{\rm d}_h,\mathrm{curl}(\boldsymbol{\varphi}-\boldsymbol{\varphi}_h))_{\mathcal{T}_h} \;-\; \langle\mathrm{curl}(\boldsymbol{\varphi}-\boldsymbol{\varphi}_h)\boldsymbol{n},\mathbf{g}\rangle_\Gamma\,.$$

The following two lemmas provide suitable upper bounds for $|\mathcal{R}_1(\boldsymbol{\zeta})|$ and $|\mathcal{R}_2(\boldsymbol{\varphi})|$.

Lemma 4.2. *There exists $C_1 > 0$, independent of h, such that*

$$|\mathcal{R}_1(\boldsymbol{\zeta})| \;\leq\; C_1 \left\{ \sum_{T \in \mathcal{T}_h} \theta_{1,T}^2 \right\}^{1/2} \|\boldsymbol{\tau}\|_{\mathbf{div},\Omega}\,,$$

where

$$\theta_{1,T}^2 \;:=\; h_T^2 \left\| \tfrac{1}{\nu}\,\boldsymbol{\sigma}_h^{\mathrm{d}} - \nabla \mathbf{u}_h \right\|_{0,T}^2 \;+\; \sum_{F \in \partial T \cap \mathcal{E}_h^i} h_F \left\| [\![\mathbf{u}_h \otimes \boldsymbol{n}]\!] \right\|_{0,F}^2 \;+\; \sum_{F \in \partial T \cap \mathcal{E}_h^\partial} h_F \left\| \mathbf{g} - \mathbf{u}_h \right\|_{0,F}^2 .$$

Proof. First, using the fact that $(\boldsymbol{\zeta} - \boldsymbol{\zeta}_h) \in \mathbb{H}^1(\Omega)$, it follows that $(\boldsymbol{\zeta} - \boldsymbol{\zeta}_h) \in \mathbb{L}^2(\mathcal{E}_h)$, whence, integrating by parts the second term in the definition of $\mathcal{R}_1$ on each $T \in \mathcal{T}_h$, we obtain that

$$\begin{aligned} \mathcal{R}_1(\boldsymbol{\zeta}) \;&=\; \frac{1}{\nu}\,(\boldsymbol{\sigma}_h^{\mathrm{d}}, \boldsymbol{\zeta} - \boldsymbol{\zeta}_h)_{\mathcal{T}_h} \;+\; \sum_{T \in \mathcal{T}_h} \left\{ -\int_T \nabla \mathbf{u}_h : (\boldsymbol{\zeta} - \boldsymbol{\zeta}_h) \;+\; \int_{\partial T} (\boldsymbol{\zeta} - \boldsymbol{\zeta}_h)\boldsymbol{n} \cdot \mathbf{u}_h \right\} \;-\; \int_\Gamma (\boldsymbol{\zeta} - \boldsymbol{\zeta}_h)\boldsymbol{n} \cdot \mathbf{g}\,, \\ &=\; (\tfrac{1}{\nu}\,\boldsymbol{\sigma}_h^{\mathrm{d}} - \nabla_h \mathbf{u}_h, \boldsymbol{\zeta} - \boldsymbol{\zeta}_h)_{\mathcal{T}_h} \;+\; \sum_{F \in \mathcal{E}_h^i} \int_F (\boldsymbol{\zeta} - \boldsymbol{\zeta}_h) : [\![\mathbf{u}_h \otimes \boldsymbol{n}]\!] \;-\; \int_\Gamma (\boldsymbol{\zeta} - \boldsymbol{\zeta}_h)\boldsymbol{n} \cdot (\mathbf{g} - \mathbf{u}_h)\,. \end{aligned}$$

Then, applying the Cauchy-Schwarz inequality in each term of the above expression, along with the estimates (4.5) and (4.6), the fact that the numbers of elements in $\Delta(T)$ and $\Delta(F)$ are bounded, and the estimate (4.8), we conclude the proof of the lemma. □

Lemma 4.3. *Assume that $\mathbf{g} \in \mathbf{H}^1(\Gamma)$. Then there exists $C_2 > 0$, independent of h, such that*

$$|\mathcal{R}_2(\boldsymbol{\varphi})| \;\leq\; C_2 \left\{ \sum_{T \in \mathcal{T}_h} \theta_{2,T}^2 \right\}^{1/2} \|\boldsymbol{\tau}\|_{\mathbf{div},\Omega}\,,$$

where

$$\theta_{2,T}^2 \;:=\; h_T^2 \left\| \mathrm{curl}(\tfrac{1}{\nu}\boldsymbol{\sigma}_h^{\mathrm{d}}) \right\|_{0,T}^2 \;+\; \sum_{F \in \partial T \cap \mathcal{E}_h^i} h_F \left\| [\![\tfrac{1}{\nu}\boldsymbol{\sigma}_h^{\mathrm{d}} \times \boldsymbol{n}]\!] \right\|_{0,F}^2 \;+\; \sum_{F \in \partial T \cap \mathcal{E}_h^\partial} h_F \left\| (\nabla \mathbf{g} - \tfrac{1}{\nu}\boldsymbol{\sigma}_h^{\mathrm{d}}) \times \boldsymbol{n} \right\|_{0,F}^2 .$$

Proof. It follows analogously to the proof of [25, Lemma 4.3] (see also [24, Lemma 4.4]). □

Now, we are ready to establish the main result of this section.

Theorem 4.1 (Reliability)**.** *Let $(\boldsymbol{\sigma}, \mathbf{u}) \in \mathbb{H} \times \mathbf{Q}$ and $(\boldsymbol{\sigma}_h, \mathbf{u}_h) \in \mathbb{H}_h \times \mathbf{Q}_h$ be the unique solutions of* (2.4) *and* (3.3)*, respectively, and suppose that $\mathbf{g} \in \mathbf{H}^1(\Gamma)$. In addition, let $\boldsymbol{\sigma}_h^\star \in \mathbb{H}$ be the postprocessed flux given by* (4.1)*. Then, for $k \geq 1$, there exists $C_{\mathtt{rel}} > 0$, independent of h, such that*

$$\|\boldsymbol{\sigma} - \boldsymbol{\sigma}_h\|_{0,\Omega} \;+\; \|\mathbf{u} - \mathbf{u}_h\|_{0,\Omega} \;+\; \|\boldsymbol{\sigma} - \boldsymbol{\sigma}_{h,0}^\star\|_{\mathbf{div},\Omega} \;\leq\; C_{\mathtt{rel}}\boldsymbol{\theta}\,,$$

where $\boldsymbol{\theta} := \Big\{ \sum_{T \in \mathcal{T}_h} \theta_T^2 \Big\}^{1/2}$, and for each $T \in \mathcal{T}_h$

$$\begin{aligned} \theta_T^2 \;:=\; & \left\| \boldsymbol{\sigma}_h - \boldsymbol{\sigma}_{h,0}^\star \right\|_{0,T}^2 \;+\; \left\| \alpha\,\mathbf{u}_h - \mathbf{div}(\boldsymbol{\sigma}_{h,0}^\star) - \mathbf{f} \right\|_{0,T}^2 \;+\; h_T^2 \left\| \tfrac{1}{\nu}\,\boldsymbol{\sigma}_h^{\mathrm{d}} - \nabla \mathbf{u}_h \right\|_{0,T}^2 \\ & +\; h_T^2 \left\| \mathrm{curl}(\tfrac{1}{\nu}\boldsymbol{\sigma}_h^{\mathrm{d}}) \right\|_{0,T}^2 \;+\; \sum_{F \in \partial T \cap \mathcal{E}_h^i} h_F \left\{ \left\| [\![\tfrac{1}{\nu}\boldsymbol{\sigma}_h^{\mathrm{d}} \times \boldsymbol{n}]\!] \right\|_{0,F}^2 \;+\; \left\| [\![\mathbf{u}_h \otimes \boldsymbol{n}]\!] \right\|_{0,F}^2 \right\} \\ & +\; \sum_{F \in \partial T \cap \mathcal{E}_h^\partial} h_F \left\{ \left\| (\nabla \mathbf{g} - \tfrac{1}{\nu}\boldsymbol{\sigma}_h^{\mathrm{d}}) \times \boldsymbol{n} \right\|_{0,F}^2 \;+\; \left\| \mathbf{g} - \mathbf{u}_h \right\|_{0,F}^2 \right\}. \end{aligned} \tag{4.10}$$

Proof. From (4.9) and Lemmas 4.2 and 4.3, it follows that

$$\|\mathcal{R}\|_{\mathbb{H}'} \;\leq\; C\left\{\sum_{T\in\mathcal{T}_h}\left(\theta_{1,T}^2+\theta_{2,T}^2\right)\right\}^{1/2},$$

which, together with (4.2), completes the proof. □

4.2 Efficiency of the a posteriori error estimator

In this section we prove the efficiency of our *a posteriori* error estimator $\boldsymbol{\theta}$. That is, we derive suitable upper bounds for the eight terms defining the local error indicator θ_T^2 (cf. (4.10)). We begin by noting, after adding and subtracting $\boldsymbol{\sigma}$, that

$$\|\boldsymbol{\sigma}_h-\boldsymbol{\sigma}_{h,0}^{\star}\|_{0,T}^2 \;\leq\; 2\,\|\boldsymbol{\sigma}-\boldsymbol{\sigma}_h\|_{0,T}^2 \;+\; 2\,\|\boldsymbol{\sigma}-\boldsymbol{\sigma}_{h,0}^{\star}\|_{0,T}^2\,. \tag{4.11}$$

Also, using the fact that $\mathbf{f}=\alpha\,\mathbf{u}-\mathbf{div}(\boldsymbol{\sigma})$ (cf. Lemma 3.1), it follows that

$$\|\alpha\,\mathbf{u}_h-\mathbf{div}(\boldsymbol{\sigma}_{h,0}^{\star})-\mathbf{f}\|_{0,T}^2 \;\leq\; 2\alpha^2\,\|\mathbf{u}-\mathbf{u}_h\|_{0,T}^2 \;+\; 2\,\|\mathbf{div}(\boldsymbol{\sigma}-\boldsymbol{\sigma}_{h,0}^{\star})\|_{0,T}^2\,. \tag{4.12}$$

Next, the estimates for the remaining six terms defining θ_T^2 (cf. (4.10)), are given as follows.

Lemma 4.4. *There exist $C_1,C_2>0$, independent of h, such that*

$$h_T^2\,\|\mathrm{curl}(\tfrac{1}{\nu}\boldsymbol{\sigma}_h^{\mathrm{d}})\|_{0,T}^2 \;\leq\; C_1\,\|\boldsymbol{\sigma}-\boldsymbol{\sigma}_h\|_{0,T}^2 \quad\forall\; T\in\mathcal{T}_h\,, \tag{4.13}$$

and

$$h_F\big\|[\![\tfrac{1}{\nu}\boldsymbol{\sigma}_h^{\mathrm{d}}\times\boldsymbol{n}]\!]\big\|_{0,F}^2 \;\leq\; C_2\,\|\boldsymbol{\sigma}-\boldsymbol{\sigma}_h\|_{0,\omega_F}^2 \quad\forall\; F\in\mathcal{E}_h^i\,, \tag{4.14}$$

where $\omega_F:=\cup\{T\in\mathcal{T}_h\,:\,F\in\partial T\}$.

Proof. As in the proof of [25, Lemma 4.11], it suffices to apply the general results stated in [25, Lemmas 4.9 and 4.10] and [24, Lemmas 4.8 and 4.9]. □

Lemma 4.5. *There exist $C_3,C_4>0$, independent of h, such that*

$$h_T^2\,\|\tfrac{1}{\nu}\,\boldsymbol{\sigma}_h^{\mathrm{d}}-\nabla\mathbf{u}_h\|_{0,T}^2 \;\leq\; C_3\Big\{h_T^2\|\boldsymbol{\sigma}-\boldsymbol{\sigma}_h\|_{0,T}^2 \;+\; \|\mathbf{u}-\mathbf{u}_h\|_{0,T}^2\Big\} \quad\forall\; T\in\mathcal{T}_h\,, \tag{4.15}$$

and

$$h_F\big\|\mathbf{g}-\mathbf{u}_h\big\|_{0,F}^2 \;\leq\; C_4\Big\{h_T^2\|\boldsymbol{\sigma}-\boldsymbol{\sigma}_h\|_{0,T}^2 \;+\; \|\mathbf{u}-\mathbf{u}_h\|_{0,T}^2\Big\} \quad\forall\; F\in\mathcal{E}_h^{\partial}\,, \tag{4.16}$$

where T is the element of $\mathcal{T}_h$ having F on its boundary.

Proof. It follows analogously to the proofs of [25, Lemmas 4.13 and 4.14]. □

Lemma 4.6. *Assume that $\mathbf{g}$ is piecewise polynomial. Then, there exists $C_5>0$, independent of h, such that*

$$h_F\big\|\big(\nabla\mathbf{g}-\tfrac{1}{\nu}\boldsymbol{\sigma}_h^{\mathrm{d}}\big)\times\boldsymbol{n}\big\|_{0,F}^2 \;\leq\; C_5\,\|\boldsymbol{\sigma}-\boldsymbol{\sigma}_h\|_{0,T}^2 \quad\forall\; F\in\mathcal{E}_h^{\partial}\,, \tag{4.17}$$

where T is the element of $\mathcal{T}_h$ having F on its boundary.

Proof. It is a slight modification of the proof of [25, Lemma 4.15] (see also [24, Lemma 4.12]). □

Lemma 4.7. *There exists $C_6 > 0$, independent of h, such that*

$$h_F \big\| [\![\mathbf{u}_h \otimes \boldsymbol{n}]\!] \big\|_{0,F}^2 \ \leq \ C_6 \Big\{ h_T^2 \|\boldsymbol{\sigma} - \boldsymbol{\sigma}_h\|_{0,\omega_F}^2 \ + \ \|\mathbf{u} - \mathbf{u}_h\|_{0,\omega_F}^2 \Big\} \quad \forall \ F \in \mathcal{E}_h^i \,, \tag{4.18}$$

where $\omega_F := \cup \{ T \in \mathcal{T}_h \, : \, F \in \partial T \}$.

Proof. We adapt the proof of [25, Lemma 4.14]. Indeed, given $F \in \mathcal{E}_h^i$ such that $F = \overline{T}^+ \cap \overline{T}^-$ (i.e. $\omega_F = \{T^+, T^-\}$), we know from Lemma 3.1 that $[\![\mathbf{u} \otimes \boldsymbol{n}]\!] = \mathbf{0}$ on F. Thus, it follows

$$\begin{aligned} h_F \big\| [\![\mathbf{u}_h \otimes \boldsymbol{n}]\!] \big\|_{0,F}^2 &= h_F \big\| [\![(\mathbf{u} - \mathbf{u}_h) \otimes \boldsymbol{n}]\!] \big\|_{0,F}^2 \\ &\leq 2h_F \|(\mathbf{u}^+ - \mathbf{u}_h^+) \otimes \boldsymbol{n}^+\|_{0,F}^2 \ + \ 2h_F \|(\mathbf{u}^- - \mathbf{u}_h^-) \otimes \boldsymbol{n}^-\|_{0,F}^2 \\ &= 2 \sum_{T \in \omega_F} h_F \|(\mathbf{u} - \mathbf{u}_h) \otimes \boldsymbol{n}\|_{0,F}^2 \ \leq \ 2 \sum_{T \in \omega_F} h_F \|\mathbf{u} - \mathbf{u}_h\|_{0,F}^2 \,. \end{aligned}$$

Next, applying a discrete-trace inequality (see, e.g. [25, eq. (4.34)]), adding and subtracting $\frac{1}{\nu} \boldsymbol{\sigma}_h^{\mathrm{d}}$, and the fact that $\nabla \mathbf{u} = \frac{1}{\nu} \boldsymbol{\sigma}^{\mathrm{d}}$ (cf. Lemma 3.1), we deduce that

$$\begin{aligned} h_F \big\| [\![\mathbf{u}_h \otimes \boldsymbol{n}]\!] \big\|_{0,F}^2 &\leq C \sum_{T \in \omega_F} \Big\{ \|\mathbf{u} - \mathbf{u}_h\|_{0,T}^2 \ + \ h_F^2 \|\nabla \mathbf{u} - \nabla \mathbf{u}_h\|_{0,T}^2 \Big\} \\ &= C \sum_{T \in \omega_F} \Big\{ \|\mathbf{u} - \mathbf{u}_h\|_{0,T}^2 \ + \ h_F^2 \|\tfrac{1}{\nu} \boldsymbol{\sigma}^{\mathrm{d}} - \tfrac{1}{\nu} \boldsymbol{\sigma}_h^{\mathrm{d}} + \tfrac{1}{\nu} \boldsymbol{\sigma}_h^{\mathrm{d}} - \nabla \mathbf{u}_h\|_{0,T}^2 \Big\} \\ &\leq C \sum_{T \in \omega_F} \Big\{ \|\mathbf{u} - \mathbf{u}_h\|_{0,T}^2 \ + \ h_T^2 \, \|\boldsymbol{\sigma} - \boldsymbol{\sigma}_h\|_{0,T}^2 \ + \ h_T^2 \, \|\tfrac{1}{\nu} \boldsymbol{\sigma}_h^{\mathrm{d}} - \nabla \mathbf{u}_h\|_{0,T}^2 \Big\} \,. \end{aligned}$$

Finally, using (4.15) in the previous estimate, we arrive to (4.18) and complete the proof. □

We end this section by establishing the efficiency of our *a posteriori* indicator $\boldsymbol{\theta}$ (cf. (4.10)).

Theorem 4.2 (Efficiency)**.** *Let $(\boldsymbol{\sigma}, \mathbf{u}) \in \mathbb{H} \times \mathbf{Q}$ and $(\boldsymbol{\sigma}_h, \mathbf{u}_h) \in \mathbb{H}_h \times \mathbf{Q}_h$ be the unique solutions of* (2.4) *and* (3.3)*, respectively, and suppose that $\mathbf{g} \in \mathbf{H}^1(\Gamma)$. In addition, let $\boldsymbol{\sigma}_h^\star \in \mathbb{H}$ be the postprocessed flux given by* (4.1)*. Then, there exists $C_{\mathtt{eff}} > 0$, independent of h, such that*

$$C_{\mathtt{eff}} \boldsymbol{\theta} \ + \ h.o.t. \ \leq \ \|\boldsymbol{\sigma} - \boldsymbol{\sigma}_h\|_{0,\Omega} \ + \ \|\mathbf{u} - \mathbf{u}_h\|_{0,\Omega} \ + \ \|\boldsymbol{\sigma} - \boldsymbol{\sigma}_{h,0}^\star\|_{\mathbf{div},\Omega} \,, \tag{4.19}$$

where h.o.t. stands for one or several terms of higher order.

Proof. It follows from estimates (4.11) up to (4.18), after summing up over $T \in \mathcal{T}_h$. In addition, we remark here that the estimate (4.17) is valid when $\mathbf{g}$ is a piecewise polynomial. Otherwise, if $\mathbf{g}$ is sufficiently smooth, then higher order terms (*h.o.t.*) would appear in (4.19). □

5 Numerical results

In this section we present three numerical examples illustrating the good performance of our HDG method (3.3), confirming the reliability and efficiency of the *a posteriori* error estimator $\boldsymbol{\theta}$, and showing the behaviour of the associated adaptive algorithm. For all the computations below, we set $\mathbf{S} := \mathbb{I}$, and consider polynomial degrees $k \in \{0, 1, 2, 3\}$ in Example 1, and $k \in \{0, 1, 2\}$ in Examples 2 and 3. In addition, in what follows N denotes the total number of unknowns of (3.3), whereas N_{comp} stands for

the number of unknowns effectively employed in the computations (involved in the resolution of the corresponding linear systems). More precisely, N is the total number of degrees of freedom defining $\boldsymbol{\sigma}_h$, $\mathbf{u}_h$, and $\boldsymbol{\lambda}_h$. On the other hand, as is natural in the HDG implementations, we can reduce N to $N_{\rm comp}$, where in the case of (3.3), $N_{\rm comp}$ is the total number of degrees of freedom defining $\boldsymbol{\lambda}_h$, plus one constant for each $T \in \mathcal{T}_h$, which has the task of imposing the condition $(\mathrm{tr}(\boldsymbol{\sigma}_h), 1)_\Omega = 0$ (see [26, Section 5] for details). In turn, the individual and total errors are defined by

$$\mathtt{e}(\boldsymbol{\sigma}) \, := \, \|\boldsymbol{\sigma} - \boldsymbol{\sigma}_h\|_{0,\Omega} \, , \quad \mathtt{e}(\mathbf{u}) \, := \, \|\mathbf{u} - \mathbf{u}_h\|_{0,\Omega} \, , \quad \mathtt{e}(\boldsymbol{\lambda}) \, := \, \left\{ \sum_{F \in \mathcal{E}_h} h_F \|\mathbf{u} - \widehat{\mathbf{u}}_h\|^2_{0,F} \right\}^{1/2} ,$$

$$\mathtt{e}(p) \, := \, \|p - p_h\|_{0,\Omega} \quad \text{and} \quad \mathtt{e}(\boldsymbol{\sigma}, \mathbf{u}) \, := \, \left\{ [\mathtt{e}(\boldsymbol{\sigma})]^2 \, + \, [\mathtt{e}(\mathbf{u})]^2 \right\}^{1/2} ,$$

where p_h is computed by the postprocessing formulae (3.11). Now, letting $\boldsymbol{\sigma}^\star_h \in \mathbb{H}(\mathbf{div}; \Omega)$ be the postprocessed flux defined by (4.1), the effectivity index with respect to $\boldsymbol{\theta}$ is given by

$$\mathtt{eff}(\boldsymbol{\theta}) \, := \, \left\{ [\mathtt{e}(\boldsymbol{\sigma}, \mathbf{u})]^2 \, + \, \|\boldsymbol{\sigma} - \boldsymbol{\sigma}^\star_{h,0}\|^2_{\mathbf{div},\Omega} \right\}^{1/2} / \, \boldsymbol{\theta} \, ,$$

and the experimental rates of convergence are defined as

$$\mathtt{r}(\cdot) \, := \, \begin{cases} \dfrac{\log\big(\mathtt{e}(\cdot) \, / \, \mathtt{e}'(\cdot)\big)}{\log(h \, / \, h')} & \text{for the quasi-uniform algorithm,} \\ \dfrac{\log\big(\mathtt{e}(\cdot) \, / \, \mathtt{e}'(\cdot)\big)}{-\frac{1}{2}\log(N \, / \, N')} & \text{for the adaptive algorithm,} \end{cases}$$

where $\mathtt{e}$ and $\mathtt{e}'$ denote the corresponding errors for two consecutive triangulations with sizes h and h', respectively. In addition, N and N' denote the corresponding total degrees of freedom of each triangulation.

The numerical results presented below were obtained using a C++ code. The corresponding linear systems arising from (3.3) are solved using the Conjugate Gradient method as the main solver. In addition, for the adaptive 3D mesh generation (cf. Example 3), we use the software TetGen developed in [35]. The examples to be considered in this section are described next. Example 1 is employed to illustrate the performance of the HDG scheme (3.3) and to confirm the reliability and efficiency of the *a posteriori* error estimator $\boldsymbol{\theta}$. Examples 2 and 3 are utilized to show the behaviour of the associated adaptive algorithm, which applies the following procedure:

(1) Start with a coarse mesh $\mathcal{T}_h$.

(2) Solve the discrete problem (3.3) for the actual mesh $\mathcal{T}_h$.

(3) Compute θ_T (cf. (4.10)) for each triangle $T \in \mathcal{T}_h$.

(4) Evaluate stopping criterion and decide to finish or go to next step.

(5) Use *red-green-blue* procedure (cf. [37]) to refine each $T' \in \mathcal{T}_h$ whose indicator $\theta_{T'}$ satisfies

$$\theta_{T'} \, \geq \, \frac{1}{2} \max\{\theta_T \, : \, T \in \mathcal{T}_h\} \, .$$

(6) Define the new mesh as actual mesh $\mathcal{T}_h$ and go to step 2.

In **Example 1** we consider $\Omega :=]0,1[^2$, $\nu = 0.1$, $\alpha = 0.5$, and choose the data $\mathbf{f}$ and $\mathbf{g}$ so that the exact solution is given by

$$\mathbf{u}(\mathbf{x}) \;:=\; \mathrm{curl}\big((x_1^2+x_2^2)\sin(2\pi x_1^2)\cos(2\pi x_2^2)\big)\,,$$

and

$$p(\mathbf{x}) \;:=\; \left(\frac{x_1^2}{9} \,+\, \frac{x_2^2}{16}\right)\sin(\pi x_1)\sin(\pi x_2) \;-\; \frac{25(\pi^2-4)}{72\pi^4}\,,$$

for all $\mathbf{x} := (x_1,x_2)^{\mathtt{t}} \in \Omega$, where $\mathrm{curl}(q) := (\partial_y q, -\partial_x q)^{\mathtt{t}}$. In Table 5.1, we summarize the convergence history of the HDG scheme (3.3) as applied to Example 1, for a sequence of quasi-uniform triangulations of $\overline{\Omega}$. We notice there that the rate of convergence $O(h^{k+1})$ predicted by Theorem 3.3 is attained by all the unknowns. In this case, we can also observe the good behaviour of the *a posteriori* error estimator $\boldsymbol{\theta}$, even for $k=0$, which is a polynomial degree not guaranteed in the reliability of $\boldsymbol{\theta}$ (cf. Theorem 4.1). In fact, we see that the effectivity index $\mathtt{eff}(\boldsymbol{\theta})$ remains always in the neighborhood of 0.31, 0.21, 0.14, and 0.10 for $k \in \{0,1,2,3\}$, respectively, which illustrates the reliability and efficiency result provided by Theorems 4.1 and 4.2.

k	h	N	N_{comp}	$\mathtt{e}(\boldsymbol{\sigma})$	$\mathtt{r}(\boldsymbol{\sigma})$	$\mathtt{e}(\mathbf{u})$	$\mathtt{r}(\mathbf{u})$	$\mathtt{e}(\boldsymbol{\lambda})$	$\mathtt{r}(\boldsymbol{\lambda})$	$\mathtt{e}(p)$	$\mathtt{r}(p)$	$\mathtt{e}(\boldsymbol{\sigma},\mathbf{u})$	$\mathtt{r}(\boldsymbol{\sigma},\mathbf{u})$	$\mathtt{eff}(\boldsymbol{\theta})$
	0.0500	14480	6481	1.79e-0	−−	7.55e-1	−−	1.57e-0	−−	8.40e-1	−−	1.95e-0	−−	0.3406
	0.0250	57760	25761	9.45e-1	0.92	3.90e-1	0.95	7.89e-1	0.99	4.62e-1	0.86	1.02e-0	0.93	0.3244
0	0.0167	129840	57841	6.41e-1	0.96	2.63e-1	0.97	5.28e-1	0.99	3.17e-1	0.93	6.93e-1	0.96	0.3197
	0.0125	230720	102721	4.85e-1	0.97	1.98e-1	0.98	3.97e-1	0.99	2.41e-1	0.95	5.23e-1	0.97	0.3175
	0.0100	360400	160401	3.90e-1	0.98	1.59e-1	0.99	3.18e-1	0.99	1.95e-1	0.96	4.21e-1	0.98	0.3162
	0.0500	38560	11361	1.09e-1	−−	5.69e-2	−−	9.85e-2	−−	3.83e-2	−−	1.23e-1	−−	0.2231
	0.0250	153920	45121	2.75e-2	1.99	1.43e-2	1.99	2.44e-2	2.02	9.32e-3	2.04	3.10e-2	1.99	0.2184
1	0.0167	346080	101281	1.23e-2	1.99	6.39e-3	1.99	1.08e-2	2.01	4.10e-3	2.03	1.38e-2	1.99	0.2166
	0.0125	615040	179841	6.90e-3	2.00	3.60e-3	2.00	6.05e-3	2.01	2.29e-3	2.02	7.78e-3	2.00	0.2157
	0.0100	960800	280801	4.42e-3	2.00	2.30e-3	2.00	3.87e-3	2.01	1.46e-3	2.01	4.99e-3	2.00	0.2151
	0.0500	72240	16241	5.26e-3	−−	2.77e-3	−−	5.24e-3	−−	1.69e-3	−−	5.94e-3	−−	0.1523
	0.0250	288480	64481	6.60e-4	2.99	3.50e-4	2.98	6.44e-4	3.02	2.07e-4	3.03	7.47e-4	2.99	0.1489
2	0.0167	648720	144721	1.96e-4	3.00	1.04e-4	2.99	1.90e-4	3.01	6.09e-5	3.02	2.22e-4	3.00	0.1479
	0.0125	1152960	256961	8.26e-5	3.00	4.39e-5	2.99	7.99e-5	3.01	2.56e-5	3.01	9.36e-5	3.00	0.1474
	0.0100	1801200	401201	4.23e-5	3.00	2.25e-5	3.00	4.08e-5	3.01	1.31e-5	3.01	4.79e-5	3.00	0.1472
	0.0500	115520	21121	2.03e-4	−−	1.06e-4	−−	2.08e-4	−−	6.26e-5	−−	2.29e-4	−−	0.1108
	0.0250	461440	83841	1.28e-5	3.99	6.73e-6	3.98	1.30e-5	4.01	3.90e-6	4.00	1.45e-5	3.99	0.1091
3	0.0167	1037760	188161	2.53e-6	4.00	1.33e-6	3.99	2.56e-6	4.01	7.69e-7	4.01	2.86e-6	3.99	0.1085
	0.0125	1844480	334081	8.02e-7	4.00	4.22e-7	4.00	8.08e-7	4.00	2.43e-7	4.01	9.06e-7	4.00	0.1082
	0.0100	2881600	521601	3.29e-7	4.00	1.73e-7	4.00	3.31e-7	4.00	9.95e-8	4.00	3.71e-7	4.00	0.1081

Table 5.1: Example 1, quasi-uniform scheme.

Next, in **Example 2** we consider the L-shaped domain $\Omega :=]-1,1[^2 \setminus [0,1]^2$, $\nu = \alpha = 1$, and choose $\mathbf{f}$ and $\mathbf{g}$ so that the exact solution is given for each $\mathbf{x} := (x_1,x_2)^{\mathtt{t}} \in \Omega$ by

$$\mathbf{u}(\mathbf{x}) \;:=\; \left(\frac{(x_2-0.1)^3}{r}, -\frac{(x_1-0.1)^3}{r}\right)^{\mathtt{t}},$$

and

$$p(\mathbf{x}) \;:=\; \frac{x_2}{x_1+1.1} \;+\; \frac{x_1}{x_2+1.1} \;+\; \frac{1}{3}\ln\left(\frac{21}{11}\right),$$

where $r := \big((x_1-0.1)^4 + (x_2-0.1)^4\big)^{4/5}$. Note that $\mathbf{u}$ is singular at $(0.1,0.1)$, and p is singular along the lines $x_1 = -1.1$ and $x_2 = -1.1$. Hence, we should expect regions of high gradients around the origin, which is the middle corner of the L, and along the lines $x_1 = -1$ and $x_2 = -1$. On the other hand, in Tables 5.2 and 5.3, we provide the convergence history of the quasi-uniform and adaptive schemes as applied to Examples 2. The stopping criterion corresponds to a maximum of 15 iterations. We observe here, as expected, that the errors of the adaptive methods decrease faster than those obtained by the quasi-uniform ones. This fact is better illustrated in Figure 5.1, where we

display the errors $\mathtt{e}(\boldsymbol{\sigma},\mathbf{u})$ vs. the degrees of freedom N for both refinements. Note that the effectivity indices (even for $k=0$) remain again bounded from above and below, which confirms the reliability and efficiency of $\boldsymbol{\theta}$ for the associated adaptive algorithm as well. Some intermediate meshes obtained with this procedure are displayed in Figure 5.2. Notice here that the adapted meshes concentrate the refinements around the origin and the lines $x_1=-1$ and $x_2=-1$, which means that the method is in fact able to recognize the regions with high gradients of the solutions.

Finally, in **Example 3** we consider the non-convex three dimensional domain

$$\Omega \;:=\;]-1,0[\times]-1,1[\times]-1,0[\;\cup\;]0,1[\times]-1,0[\times]-1,0[\;\cup\;]-1,0[\times]-1,0[\times]0,1[\,,$$

with $\nu=0.5$, $\alpha=100$, and choose the data $\mathbf{f}$ and $\mathbf{g}$ so that the exact solution is given for each $\mathbf{x}:=(x_1,x_2,x_3)^{\mathtt{t}}\in\Omega$ by

$$\mathbf{u}(\mathbf{x}) \;:=\; \left(\frac{x_2-x_3}{r},\,\frac{x_3-x_1}{r},\,\frac{x_1-x_2}{r}\right)^{\mathtt{t}},$$

and

$$p(\mathbf{x}) \;:=\; (x_1+1)\,(x_2+1)\,(x_3+1)\,e^{x_1+x_2+x_3} \;-\; \frac{e^{-3}}{4}(3e^2+1)\,,$$

where $r:=\sqrt{(x_1-0.01)^2+(x_2-0.01)^2+(x_3-0.01)^2}$. As in Example 2, here $\mathbf{u}$ is singular at $(0.01,0.01,0.01)$, and then we should expect regions of high gradients around the origin. Similar as before, we present the convergence history for Example 3 in Tables 5.4 and 5.5, where, we see the limited regularity of $\mathbf{u}$ in the rates of convergence. Now, the stopping criterion corresponds to a maximum of 10 iterations, and we display the errors $\mathtt{e}(\boldsymbol{\sigma},\mathbf{u})$ vs. N, for both refinements, in Figure 5.3. There, for $k=0$, we can appreciate that the errors of the adaptive scheme is not faster than the quasi-uniform method, which could correspond to either a special feature of Example 3 or the fact that $k=0$ is not covered in Theorem 4.1. Some intermediate meshes obtained with this procedure are displayed in Figure 5.4. Once again, we notice that the adapted meshes concentrate the refinements around the regions with high gradients of the solutions.

We end this section by displaying, in Figures 5.5, 5.6 and 5.7, some components of the discrete solutions for the three examples, in order to illustrate resolution of the HDG method (3.3).

k	h	N	N_{comp}	$\mathtt{e}(\boldsymbol{\sigma})$	$\mathtt{r}(\boldsymbol{\sigma})$	$\mathtt{e}(\mathbf{u})$	$\mathtt{r}(\mathbf{u})$	$\mathtt{e}(\boldsymbol{\lambda})$	$\mathtt{r}(\boldsymbol{\lambda})$	$\mathtt{e}(p)$	$\mathtt{r}(p)$	$\mathtt{e}(\boldsymbol{\sigma},\mathbf{u})$	$\mathtt{r}(\boldsymbol{\sigma},\mathbf{u})$	$\mathtt{eff}(\boldsymbol{\theta})$
	0.1414	5480	2481	2.07e-0	−−	8.78e-1	−−	2.40e-1	−−	7.12e-1	−−	2.25e-0	−−	0.9905
	0.0566	33950	15201	9.42e-1	0.86	4.04e-1	0.85	9.61e-2	1.00	3.32e-1	0.83	1.02e-0	0.86	0.9907
	0.0354	86720	38721	6.02e-1	0.95	2.60e-1	0.94	5.97e-2	1.01	2.09e-1	0.99	6.55e-1	0.95	0.9898
0	0.0257	163790	73041	4.41e-1	0.97	1.91e-1	0.97	4.33e-2	1.01	1.52e-1	0.99	4.81e-1	0.97	0.9893
	0.0202	265160	118161	3.48e-1	0.98	1.51e-1	0.98	3.39e-2	1.01	1.20e-1	0.99	3.79e-1	0.98	0.9890
	0.0166	390830	174081	2.87e-1	0.99	1.25e-1	0.99	2.79e-2	1.01	9.87e-2	0.99	3.13e-1	0.99	0.9888
	0.0141	540800	240801	2.44e-1	0.99	1.06e-1	0.99	2.37e-2	1.01	8.39e-2	0.99	2.66e-1	0.99	0.9887
	0.1414	14560	4361	7.19e-1	−−	2.46e-1	−−	5.07e-2	−−	2.35e-1	−−	7.60e-1	−−	0.9713
	0.0566	90400	26651	1.54e-1	1.68	5.87e-2	1.56	8.50e-3	1.95	4.59e-2	1.78	1.65e-1	1.67	0.9815
	0.0354	231040	67841	6.48e-2	1.84	2.47e-2	1.84	3.39e-3	1.96	1.92e-2	1.85	6.94e-2	1.84	0.9804
1	0.0257	436480	127931	3.50e-2	1.93	1.34e-2	1.93	1.80e-3	1.98	1.02e-2	2.00	3.75e-2	1.93	0.9805
	0.0202	706720	206921	2.18e-2	1.96	8.35e-3	1.95	1.11e-3	1.99	6.25e-3	2.02	2.34e-2	1.96	0.9806
	0.0166	1041760	304811	1.49e-2	1.97	5.70e-3	1.97	7.57e-4	2.00	4.22e-3	2.02	1.59e-2	1.97	0.9806
	0.0141	1441600	421601	1.08e-2	1.98	4.13e-3	1.98	5.47e-4	2.00	3.04e-3	2.02	1.15e-2	1.98	0.9806
	0.1414	27240	6241	2.41e-1	−−	7.80e-2	−−	1.47e-2	−−	6.37e-2	−−	2.53e-1	−−	0.9700
	0.0566	169350	38101	3.23e-2	2.19	1.11e-2	2.12	1.19e-3	2.74	1.02e-2	2.00	3.42e-2	2.18	0.9631
	0.0354	432960	96961	8.62e-3	2.81	2.93e-3	2.84	3.19e-4	2.80	2.72e-3	2.82	9.11e-3	2.82	0.9671
2	0.0257	818070	182821	3.45e-3	2.87	1.17e-3	2.87	1.26e-4	2.92	1.10e-3	2.85	3.65e-3	2.87	0.9682
	0.0202	1324680	295681	1.71e-3	2.92	5.80e-4	2.92	6.18e-5	2.95	5.45e-4	2.90	1.80e-3	2.92	0.9685
	0.0166	1952790	435541	9.62e-4	2.95	3.27e-4	2.95	3.47e-5	2.97	3.08e-4	2.94	1.02e-3	2.95	0.9685
	0.0141	2702400	602401	5.94e-4	2.96	2.02e-4	2.96	2.14e-5	2.98	1.91e-4	2.96	6.28e-4	2.96	0.9685

Table 5.2: Example 2, quasi-uniform scheme.

k	h	N	N_{comp}	$\mathtt{e}(\boldsymbol{\sigma})$	$\mathtt{r}(\boldsymbol{\sigma})$	$\mathtt{e}(\mathbf{u})$	$\mathtt{r}(\mathbf{u})$	$\mathtt{e}(\boldsymbol{\lambda})$	$\mathtt{r}(\boldsymbol{\lambda})$	$\mathtt{e}(p)$	$\mathtt{r}(p)$	$\mathtt{e}(\boldsymbol{\sigma},\mathbf{u})$	$\mathtt{r}(\boldsymbol{\sigma},\mathbf{u})$	$\mathtt{eff}(\boldsymbol{\theta})$
	0.1414	5480	2481	2.07e-0	−−	8.78e-1	−−	2.40e-1	−−	7.12e-1	−−	2.25e-0	−−	0.9905
	0.1414	5570	2521	2.03e-0	2.14	8.07e-1	10.32	2.24e-1	8.23	7.70e-1	-9.76	2.19e-0	3.32	0.9861
	0.1414	5718	2589	1.74e-0	11.76	7.08e-1	10.02	2.13e-1	4.02	7.11e-1	6.07	1.88e-0	11.52	0.9850
	0.1414	6206	2807	1.54e-0	2.99	6.03e-1	3.91	1.90e-1	2.75	6.66e-1	1.62	1.66e-0	3.12	0.9844
	0.1414	6810	3081	1.39e-0	2.29	5.62e-1	1.52	1.81e-1	1.04	6.25e-1	1.36	1.50e-0	2.19	0.9801
	0.1414	7694	3475	1.29e-0	1.19	5.13e-1	1.50	1.77e-1	0.35	5.81e-1	1.20	1.39e-0	1.23	0.9756
	0.1414	9544	4305	1.11e-0	1.36	4.52e-1	1.17	1.57e-1	1.11	5.16e-1	1.10	1.20e-0	1.33	0.9753
0	0.1414	13456	6057	9.44e-1	0.96	3.74e-1	1.11	1.43e-1	0.57	4.41e-1	0.92	1.02e-0	0.98	0.9706
	0.1414	20528	9219	7.81e-1	0.90	3.07e-1	0.93	1.27e-1	0.56	3.70e-1	0.82	8.39e-1	0.90	0.9674
	0.1414	32598	14614	6.56e-1	0.76	2.54e-1	0.82	1.10e-1	0.63	3.11e-1	0.75	7.03e-1	0.76	0.9629
	0.1414	58320	26081	4.99e-1	0.94	1.93e-1	0.95	8.63e-2	0.82	2.38e-1	0.92	5.34e-1	0.94	0.9630
	0.1414	89106	39817	4.03e-1	1.00	1.57e-1	0.96	7.08e-2	0.93	1.93e-1	0.99	4.33e-1	0.99	0.9637
	0.1414	162650	72566	3.03e-1	0.95	1.16e-1	1.00	5.15e-2	1.06	1.47e-1	0.91	3.25e-1	0.95	0.9637
	0.1000	257440	114771	2.43e-1	0.97	9.35e-2	0.95	4.14e-2	0.96	1.18e-1	0.96	2.60e-1	0.97	0.9632
	0.1000	460856	205317	1.80e-1	1.03	6.97e-2	1.01	3.07e-2	1.02	8.71e-2	1.03	1.93e-1	1.03	0.9643
	0.1414	14560	4361	7.19e-1	−−	2.46e-1	−−	5.07e-2	−−	2.35e-1	−−	7.60e-1	−−	0.9713
	0.1414	14800	4431	5.00e-1	44.40	1.59e-1	53.09	3.94e-2	30.85	1.91e-1	25.37	5.25e-1	45.25	0.9841
	0.1414	15192	4551	3.55e-1	26.33	1.22e-1	20.49	2.89e-2	23.71	1.28e-1	30.68	3.75e-1	25.75	0.9787
	0.1414	15436	4625	3.13e-1	15.62	1.17e-1	5.59	2.47e-2	19.70	1.14e-1	13.90	3.34e-1	14.48	0.9653
	0.1414	17076	5109	2.39e-1	5.36	9.03e-2	5.06	1.82e-2	6.04	9.95e-2	2.74	2.55e-1	5.33	0.9580
	0.1414	18528	5541	1.98e-1	4.58	7.36e-2	5.02	1.47e-2	5.26	8.78e-2	3.09	2.11e-1	4.63	0.9442
	0.1414	22372	6665	1.41e-1	3.64	5.20e-2	3.68	1.25e-2	1.70	6.13e-2	3.81	1.50e-1	3.65	0.9333
1	0.1414	26960	8023	1.11e-1	2.57	4.16e-2	2.39	1.11e-2	1.33	4.95e-2	2.29	1.18e-1	2.55	0.9241
	0.1414	37476	11127	7.58e-2	2.29	2.89e-2	2.23	8.13e-3	1.87	3.39e-2	2.30	8.11e-2	2.28	0.9197
	0.1414	46632	13823	6.01e-2	2.12	2.27e-2	2.20	7.24e-3	1.05	2.62e-2	2.36	6.43e-2	2.13	0.9098
	0.1414	68048	20109	4.19e-2	1.91	1.61e-2	1.82	5.07e-3	1.89	1.83e-2	1.90	4.49e-2	1.90	0.9011
	0.1414	108460	31995	2.72e-2	1.86	1.03e-2	1.90	3.38e-3	1.74	1.19e-2	1.84	2.91e-2	1.86	0.8976
	0.1414	146872	43241	2.01e-2	2.00	7.71e-3	1.93	2.69e-3	1.51	8.69e-3	2.08	2.15e-2	1.99	0.8951
	0.1414	228396	67101	1.27e-2	2.07	4.91e-3	2.05	1.74e-3	1.97	5.50e-3	2.07	1.36e-2	2.07	0.8956
	0.1000	346306	101660	8.49e-3	1.93	3.27e-3	1.94	1.11e-3	2.15	3.70e-3	1.91	9.10e-3	1.93	0.8958
	0.1414	27240	6241	2.41e-1	−−	7.80e-2	−−	1.47e-2	−−	6.37e-2	−−	2.53e-1	−−	0.9700
	0.1414	27690	6341	1.54e-1	54.47	5.63e-2	39.80	6.19e-3	105.64	4.31e-2	47.65	1.64e-1	52.92	0.9790
	0.1414	27882	6393	1.17e-1	80.93	4.69e-2	53.08	5.04e-3	59.88	4.24e-2	4.64	1.26e-1	77.36	0.9662
	0.1414	28782	6593	7.94e-2	24.12	2.90e-2	30.30	4.34e-3	9.29	2.93e-2	23.18	8.46e-2	24.91	0.9332
	0.1414	29058	6659	6.15e-2	53.49	2.36e-2	42.98	3.74e-3	31.33	2.30e-2	51.45	6.59e-2	52.20	0.9090
	0.1414	31050	7111	4.44e-2	9.84	1.65e-2	10.72	2.67e-3	10.16	1.80e-2	7.26	4.74e-2	9.95	0.8964
	0.1414	33576	7677	3.34e-2	7.30	1.17e-2	8.89	1.98e-3	7.70	1.50e-2	4.73	3.54e-2	7.48	0.8964
2	0.1414	38718	8829	2.07e-2	6.69	7.28e-3	6.63	1.36e-3	5.27	9.36e-3	6.63	2.20e-2	6.68	0.8809
	0.1414	47664	10845	1.22e-2	5.10	4.39e-3	4.87	9.45e-4	3.49	5.37e-3	5.35	1.30e-2	5.08	0.8801
	0.1414	56346	12807	9.06e-3	3.55	3.35e-3	3.22	7.22e-4	3.22	4.00e-3	3.52	9.66e-3	3.51	0.8758
	0.1414	74136	16807	5.76e-3	3.31	2.06e-3	3.57	5.26e-4	2.31	2.63e-3	3.05	6.11e-3	3.34	0.8638
	0.1414	94086	21287	4.14e-3	2.77	1.47e-3	2.85	4.11e-4	2.07	1.86e-3	2.94	4.39e-3	2.77	0.8457
	0.1414	117960	26611	2.83e-3	3.36	1.03e-3	3.14	3.00e-4	2.77	1.29e-3	3.22	3.01e-3	3.33	0.8418
	0.1414	164358	37029	1.73e-3	2.97	6.23e-4	3.02	1.77e-4	3.19	7.75e-4	3.07	1.84e-3	2.98	0.8469
	0.1414	225408	50689	1.14e-3	2.66	4.05e-4	2.72	1.22e-4	2.37	5.08e-4	2.67	1.21e-3	2.67	0.8377

Table 5.3: Example 2, adaptive scheme.

References

[1] V. Anaya, G. N. Gatica, D. Mora, and R. Ruiz-Baier, *An augmented velocity-vorticity-pressure formulation for the Brinkman equations*, Internat. J. Numer. Methods Fluids, 79 (2015), pp. 109–137.

[2] V. Anaya, D. Mora, R. Oyarzúa, and R. Ruiz-Baier, *A priori and a posteriori error analysis of a mixed scheme for the Brinkman problem*, Numer. Math., 133 (2016), pp. 781–817.

[3] V. Anaya, D. Mora, C. Reales, and R. Ruiz-Baier, *Stabilized mixed approximation of axisymmetric Brinkman flow*, ESAIM Math. Model. Numer. Anal., 49 (2015), pp. 855–874.

[4] E. Cáceres, G. N. Gatica, and F. A. Sequeira, *A mixed virtual element method for the Brinkman problem*, Math. Models Methods Appl. Sci., To appear (2017).

k	h	N	N_{comp}	$\mathtt{e}(\boldsymbol{\sigma})$	$\mathtt{r}(\boldsymbol{\sigma})$	$\mathtt{e}(\mathbf{u})$	$\mathtt{r}(\mathbf{u})$	$\mathtt{e}(\boldsymbol{\lambda})$	$\mathtt{r}(\boldsymbol{\lambda})$	$\mathtt{e}(p)$	$\mathtt{r}(p)$	$\mathtt{e}(\boldsymbol{\sigma},\mathbf{u})$	$\mathtt{r}(\boldsymbol{\sigma},\mathbf{u})$	$\mathtt{eff}(\boldsymbol{\theta})$
0	0.4330	28512	11617	1.52e-0	−−	3.01e-1	−−	5.27e-1	−−	7.47e-1	−−	1.55e-0	−−	0.4642
	0.2887	95256	38233	1.30e-0	0.40	2.07e-1	0.93	2.88e-1	1.49	6.52e-1	0.33	1.31e-0	0.41	0.5863
	0.2165	224640	89473	1.14e-0	0.45	1.61e-1	0.86	1.90e-1	1.45	5.82e-1	0.40	1.15e-0	0.46	0.6560
	0.1732	437400	173401	1.01e-0	0.54	1.34e-1	0.83	1.36e-1	1.49	5.20e-1	0.50	1.02e-0	0.54	0.6927
	0.1575	581526	230143	9.56e-1	0.57	1.23e-1	0.88	1.18e-1	1.49	4.94e-1	0.54	9.64e-1	0.58	0.7126
	0.1443	754272	298081	9.11e-1	0.56	1.13e-1	1.00	1.03e-1	1.53	4.71e-1	0.55	9.18e-1	0.56	0.7501
	0.1332	958230	378223	8.66e-1	0.64	1.05e-1	0.94	9.22e-2	1.44	4.49e-1	0.59	8.72e-1	0.65	0.7428
	0.1019	2138022	840991	7.28e-1	0.64	8.38e-2	0.83	6.16e-2	1.50	3.79e-1	0.63	7.33e-1	0.65	0.8021
	0.0912	2982582	1171807	6.74e-1	0.70	7.62e-2	0.86	5.22e-2	1.50	3.51e-1	0.69	6.78e-1	0.70	0.8146
	0.0825	4024566	1579663	6.27e-1	0.72	6.99e-2	0.86	4.49e-2	1.49	3.27e-1	0.71	6.31e-1	0.72	0.8242
1	0.4330	103968	31777	4.08e-1	−−	5.63e-2	−−	6.67e-2	−−	7.06e-2	−−	4.12e-1	−−	0.8626
	0.2887	347976	104329	2.95e-1	0.80	4.18e-2	0.73	2.92e-2	2.04	5.02e-2	0.84	2.98e-1	0.80	0.9128
	0.2165	821376	243841	2.29e-1	0.89	3.35e-2	0.78	1.65e-2	1.98	3.74e-2	1.02	2.31e-1	0.89	0.9184
	0.1732	1600200	472201	1.84e-1	0.96	2.66e-2	1.04	1.02e-2	2.17	3.36e-2	0.49	1.86e-1	0.96	0.9019
	0.1575	2127906	626539	1.68e-1	0.98	2.40e-2	1.05	8.33e-3	2.10	3.06e-2	0.96	1.70e-1	0.98	0.9033
	0.1443	2760480	811297	1.54e-1	0.98	2.19e-2	1.05	7.03e-3	1.95	2.81e-2	0.99	1.56e-1	0.98	0.9304
	0.1332	3507426	1029211	1.42e-1	1.06	1.99e-2	1.21	5.83e-3	2.34	2.60e-2	0.97	1.43e-1	1.06	0.9053
2	0.4330	244800	62017	2.58e-1	−−	3.44e-2	−−	2.61e-2	−−	5.43e-2	−−	2.61e-1	−−	0.8116
	0.2887	820368	203473	1.74e-1	0.98	2.44e-2	0.84	1.12e-2	2.09	3.39e-2	1.16	1.76e-1	0.97	0.8372
	0.2165	1937664	475393	1.28e-1	1.07	1.75e-2	1.15	6.04e-3	2.14	2.39e-2	1.22	1.29e-1	1.08	0.8298
	0.1732	3776400	920401	9.90e-2	1.14	1.22e-2	1.63	3.36e-3	2.63	2.00e-2	0.80	9.98e-2	1.15	0.8254
	0.1575	5022468	1221133	8.83e-2	1.20	1.06e-2	1.46	2.68e-3	2.35	1.78e-2	1.24	8.90e-2	1.20	0.8313
	0.1443	6516288	1581121	7.78e-2	1.46	9.39e-3	1.38	2.18e-3	2.41	1.60e-2	1.23	7.83e-2	1.46	0.8368
	0.1332	8280324	2005693	7.16e-2	1.03	8.22e-3	1.67	1.79e-3	2.44	1.44e-2	1.27	7.21e-2	1.04	0.8432

Table 5.4: Example 3, quasi-uniform scheme.

k	h	N	N_{comp}	$\mathtt{e}(\boldsymbol{\sigma})$	$\mathtt{r}(\boldsymbol{\sigma})$	$\mathtt{e}(\mathbf{u})$	$\mathtt{r}(\mathbf{u})$	$\mathtt{e}(\boldsymbol{\lambda})$	$\mathtt{r}(\boldsymbol{\lambda})$	$\mathtt{e}(p)$	$\mathtt{r}(p)$	$\mathtt{e}(\boldsymbol{\sigma},\mathbf{u})$	$\mathtt{r}(\boldsymbol{\sigma},\mathbf{u})$	$\mathtt{eff}(\boldsymbol{\theta})$
0	0.4330	28512	11617	1.52e-0	−−	3.01e-1	−−	5.27e-1	−−	7.47e-1	−−	1.55e-0	−−	0.4642
	0.4330	31260	12737	1.46e-0	0.92	2.77e-1	1.79	4.75e-1	2.23	7.55e-1	-0.24	1.49e-0	0.95	0.4373
	0.4330	33447	13637	1.43e-0	0.56	2.74e-1	0.40	4.74e-1	0.11	7.57e-1	-0.10	1.46e-0	0.56	0.3306
	0.4330	35910	14648	1.42e-0	0.21	2.71e-1	0.23	4.70e-1	0.22	7.55e-1	0.08	1.45e-0	0.21	0.2721
	0.4330	87501	35043	1.36e-0	0.09	2.02e-1	0.67	3.20e-1	0.86	7.51e-1	0.01	1.38e-0	0.11	0.3275
	0.4330	237450	94880	1.19e-0	0.28	1.46e-1	0.66	1.85e-1	1.09	6.58e-1	0.26	1.20e-0	0.28	0.3655
	0.3355	284337	113354	1.16e-0	0.27	1.33e-1	0.97	1.62e-1	1.49	6.46e-1	0.22	1.17e-0	0.28	0.3741
	0.3021	577908	228351	1.03e-0	0.34	1.03e-1	0.72	1.10e-1	1.10	5.77e-1	0.32	1.03e-0	0.34	0.4132
	0.2500	858816	338737	9.40e-1	0.45	8.97e-2	0.72	8.70e-2	1.16	5.30e-1	0.43	9.45e-1	0.45	0.4246
	0.1958	1847256	726885	7.97e-1	0.43	7.09e-2	0.62	6.05e-2	0.95	4.50e-1	0.42	8.00e-1	0.43	0.4443
1	0.4330	103968	31777	4.08e-1	−−	5.63e-2	−−	6.67e-2	−−	7.06e-2	−−	4.12e-1	−−	0.8626
	0.4330	111258	33991	2.46e-1	14.93	3.86e-2	11.18	4.29e-2	13.01	5.27e-2	8.64	2.49e-1	14.86	0.8537
	0.4330	119091	36419	1.54e-1	13.82	2.66e-2	10.94	4.12e-2	1.21	3.64e-2	10.84	1.56e-1	13.75	0.7023
	0.4330	125172	38317	1.39e-1	3.91	2.52e-2	2.23	4.11e-2	0.06	3.56e-2	0.95	1.42e-1	3.86	0.5186
	0.4330	136395	41644	1.22e-1	3.09	2.32e-2	1.84	3.88e-2	1.38	3.37e-2	1.29	1.24e-1	3.05	0.4827
	0.4330	221220	66826	7.68e-2	1.92	1.69e-2	1.32	2.72e-2	1.47	2.28e-2	1.60	7.86e-2	1.90	0.5030
	0.4330	323382	97031	5.95e-2	1.34	1.33e-2	1.26	2.14e-2	1.26	2.02e-2	0.65	6.10e-2	1.34	0.4618
	0.4330	581649	173361	4.69e-2	0.81	9.28e-3	1.23	1.34e-2	1.59	1.83e-2	0.33	4.78e-2	0.83	0.4916
	0.4330	893673	265519	3.38e-2	1.53	6.82e-3	1.43	8.72e-3	2.01	1.26e-2	1.76	3.45e-2	1.53	0.5161
	0.4330	1376466	407421	2.41e-2	1.57	5.09e-3	1.36	5.92e-3	1.79	8.37e-3	1.88	2.46e-2	1.56	0.5210
2	0.4330	244800	62017	2.58e-1	−−	3.44e-2	−−	2.61e-2	−−	5.43e-2	−−	2.61e-1	−−	0.8116
	0.4330	262458	66466	1.27e-1	20.50	1.57e-2	22.61	7.93e-3	34.24	2.68e-2	20.30	1.27e-1	20.54	0.8173
	0.4330	281232	71317	4.05e-2	33.00	4.99e-3	33.10	6.18e-3	7.23	9.57e-3	29.78	4.08e-2	33.00	0.6177
	0.4330	300072	76115	3.49e-2	4.60	4.16e-3	5.65	6.13e-3	0.21	8.74e-3	2.78	3.51e-2	4.62	0.3428
	0.4330	391806	98353	1.93e-2	4.42	2.61e-3	3.48	3.92e-3	3.35	5.41e-3	3.60	1.95e-2	4.40	0.4637
	0.4330	455064	114249	1.39e-2	4.41	2.07e-3	3.15	3.30e-3	2.32	3.62e-3	5.36	1.41e-2	4.39	0.4299
	0.4330	635082	158250	9.61e-3	2.22	1.54e-3	1.76	2.42e-3	1.85	2.61e-3	1.95	9.73e-3	2.21	0.3537
	0.4330	936180	231820	6.29e-3	2.19	1.05e-3	1.95	1.65e-3	1.99	1.83e-3	1.84	6.37e-3	2.18	0.3922
	0.4330	1467894	360362	4.09e-3	1.91	7.61e-4	1.45	1.24e-3	1.26	1.31e-3	1.48	4.16e-3	1.90	0.3649
	0.4330	2272302	556561	2.61e-3	2.05	4.58e-4	2.33	6.24e-4	3.14	9.91e-4	1.29	2.65e-3	2.06	0.3971

Table 5.5: Example 3, adaptive scheme.

[5] J. Carrero, B. Cockburn, and D. Schötzau, *Hybridized, globally divergence-free LDG methods. Part I: The Stokes problem*, Math. Comp., 75 (2006), pp. 533–563.

[6] H. Chen, J. Li, and W. Qiu, *Robust a posteriori error estimates for HDG methods for the convection-diffusion equations*, IMA J. Numer. Anal., 36 (2016), pp. 437–462.

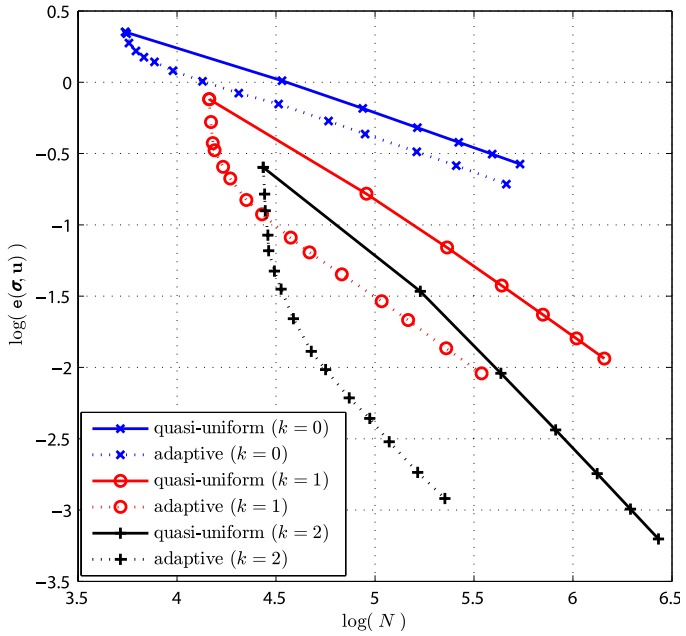

Figure 5.1: Example 2, $\mathsf{e}(\boldsymbol{\sigma}, \mathbf{u})$ vs. N.

[7] P. G. Ciarlet, *The Finite Element Method for Elliptic Problems, Studies in Mathematics and its Applications, Vol. 4*, North-Holland Publishing Co., Amsterdam-New York-Oxford, 1978.

[8] P. Clément, *Approximation by finite element functions using local regularisation*, ESAIM Math. Model. Numer. Anal., 9 (1975), pp. 77–84.

[9] B. Cockburn, B. Dong, and J. Guzmán, *A superconvergent LDG-hybridizable Galerkin method for second-order elliptic problems*, Math. Comp., 77 (2008), pp. 1887–1916.

[10] B. Cockburn, J. Gopalakrishnan, and R. Lazarov, *Unified hybridization of discontinuous Galerkin, mixed and continuous Galerkin methods for second order elliptic problems*, SIAM J. Numer. Anal., 47 (2009), pp. 1319–1365.

[11] B. Cockburn, J. Gopalakrishnan, N. C. Nguyen, J. Peraire, and F. J. Sayas, *Analysis of HDG methods for Stokes flow*, Math. Comp., 80 (2011), pp. 723–760.

[12] B. Cockburn, J. Gopalakrishnan, and F. J. Sayas, *A projection-based error analysis of HDG methods*, Math. Comp., 79 (2010), pp. 1351–1367.

[13] B. Cockburn, J. Guzmán, and H. Wang, *Superconvergent discontinuous Galerkin methods for second-order elliptic problems*, Math. Comp., 78 (2009), pp. 1–24.

[14] B. Cockburn and F.-J. Sayas, *Divergence-conforming HDG methods for Stokes flows*, Math. Comp., 83 (2014), pp. 1571–1598.

[15] B. Cockburn and K. Shi, *Superconvergent HDG methods for linear elasticity with weakly symmetric stress*, IMA J. Numer. Anal., 33 (2013), pp. 747–770.

[16] ———, *Devising HDG methods for Stokes flow: An overview*, Comput. & Fluids, 98 (2014), pp. 221–229.

[17] B. Cockburn and C. Shu, *The local discontinuous Galerkin method for the time-dependent convection-diffusion systems*, SIAM J. Numer. Anal., 35 (1998), pp. 2440–2463.

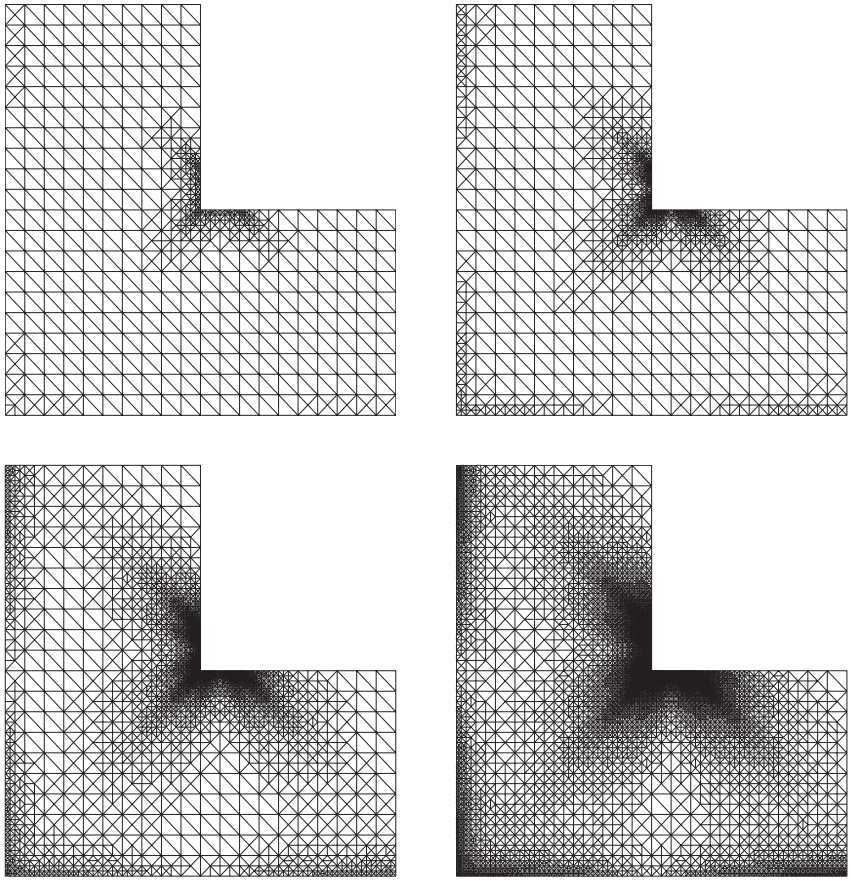

Figure 5.2: Example 2, adapted meshes for $k = 0$ with $N \in \{9544, 20528, 58320, 162650\}$.

[18] B. Cockburn and W. Zhang, *A posteriori error estimates for HDG methods*, J. Sci. Comput., 51 (2012), pp. 582–607.

[19] G. Fu, Y. Jin, and W. Qiu, *Parameter-Free superconvergent H(div)-conforming HDG methods for the Brinkman equation*, Preprint arXiv:1607.07662, (2016).

[20] G. N. Gatica, *A note on stable Helmholtz decompositions in 3D*, Preprint 2016-03, Centro de Investigación en Ingeniería Matemática (CI^2MA), Universidad de Concepción, Chile, (2016).

[21] G. N. Gatica, L. F. Gatica, and A. Márquez, *Analysis of a pseudostress-based mixed finite element method for the Brinkman model of porous media flow*, Numer. Math., 126 (2014), pp. 635–677.

[22] ——, *Analysis of a pseudostress-based mixed finite element method for the Brinkman model of porous media flow*, Numer. Math., 126 (2014), pp. 635–677.

[23] G. N. Gatica, L. F. Gatica, and F. A. Sequeira, *Analysis of an augmented pseudostress-based mixed formulation for a nonlinear Brinkman model of porous media flow*, Comput. Methods Appl. Mech. Engrg., 289 (2015), pp. 104–130.

[24] ——, *A priori and a posteriori error analyses of a pseudostress-based mixed formulation for linear elasticity*, Comput. Mat. Appl., 71 (2016), pp. 585–614.

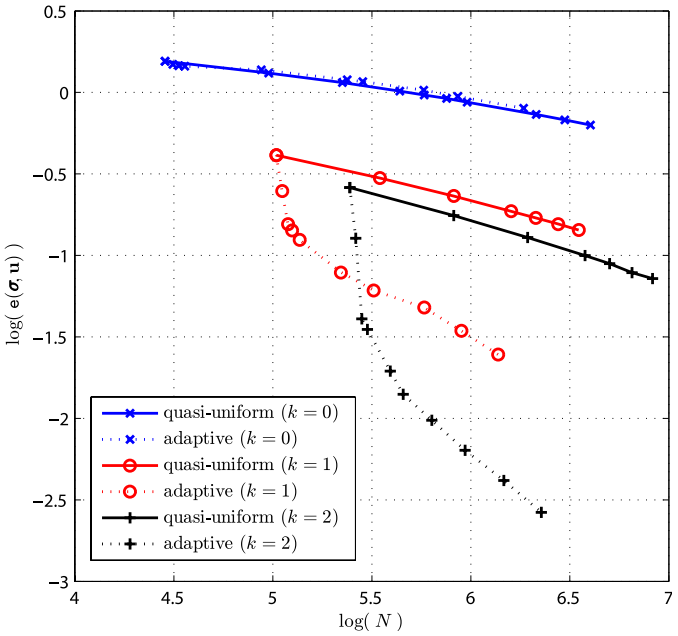

Figure 5.3: Example 3, $\mathsf{e}(\boldsymbol{\sigma}, \mathbf{u})$ vs. N.

[25] G. N. Gatica, A. Márquez, and M. A. Sánchez, *Analysis of a velocity-pressure-pseudostress formulation for the stationary Stokes equations*, Comput. Methods Appl. Mech. Engrg., 199 (2010), pp. 1064–1079.

[26] G. N. Gatica and F. A. Sequeira, *Analysis of an augmented HDG method for a class of quasi-Newtonian Stokes flows*, J. Sci. Comput., 65 (2015), pp. 1270–1308.

[27] ——, *A priori and a posteriori error analyses of an augmented HDG method for a class of quasi-Newtonian Stokes flows*, J. Sci. Comput., 69 (2016), pp. 1192–1250.

[28] ——, *Analysis of the HDG method for the Stokes-Darcy coupling*, Numer. Methods Partial Differential Equations, doi:10.1002/num.22128 (2017).

[29] V. Girault and P. A. Raviart, *Finite Element Methods for Navier-Stokes Equations. Theory and Algorithms*, Springer Series in Computational Mathematics, Vol. 5, Springer, Berlin, 1986.

[30] J. Guzmán and M. Neilan, *A family of nonconforming elements for the Brinkman problem*, IMA J. Numer. Anal., 32 (2012), pp. 1484–1508.

[31] M. Juntenen and R. Stenberg, *Analysis of finite element methods for the Brinkman problem*, Calcolo, 47 (2010), pp. 129–147.

[32] J. Könnö and R. Stenberg, *H(div)-conforming finite elements for the Brinkman problem*, Math. Models Methods Appl. Sci., 21 (2011), pp. 2227–2248.

[33] ——, *Numerical computations with H(div)-finite elements for the Brinkman problem*, Comp. Geosci., 16 (2012), pp. 139–158.

[34] N. C. Nguyen, J. Peraire, and B. Cockburn, *A hybridizable discontinuous Galerkin method for Stokes flow*, Comput. Methods Appl. Mech. Engrg., 199 (2010), pp. 582–597.

[35] H. Si, *TetGen: A Quality Tetrahedral Mesh Generator and 3D Delaunay Triangulator v.1.5 User's manual*, Tech. Report 13, Weierstrass Institute for Applied Analysis and Stochastics, Berlin, 2013.

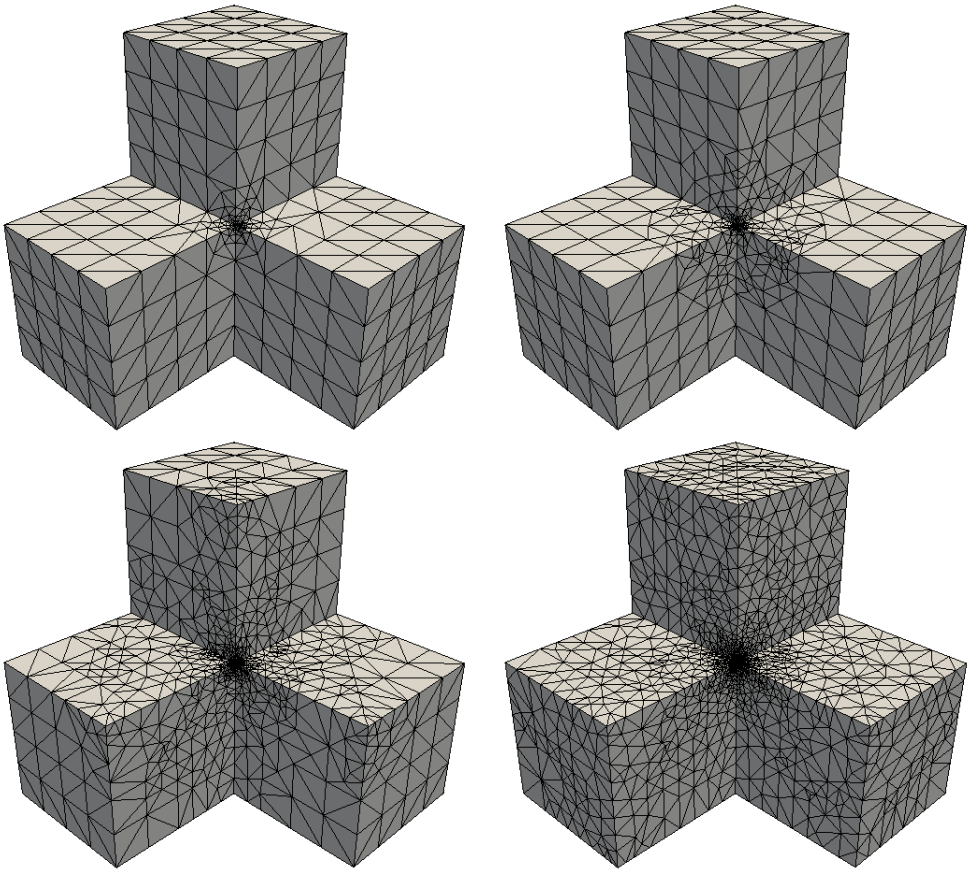

Figure 5.4: Example 3, adapted meshes for $k = 1$ with $N \in \{125172, 221220, 581649, 1376466\}$.

[36] P. S. Vassilevski and U. Villa, *A mixed formulation for the Brinkman problem*, SIAM J. Numer. Anal., 52 (2014), pp. 258–281.

[37] R. Verfürth, *A Review of A Posteriori Error Estimation and Adaptive-Mesh-Refinement Techniques*, Wiley, Teubner, Chichester, 1996.

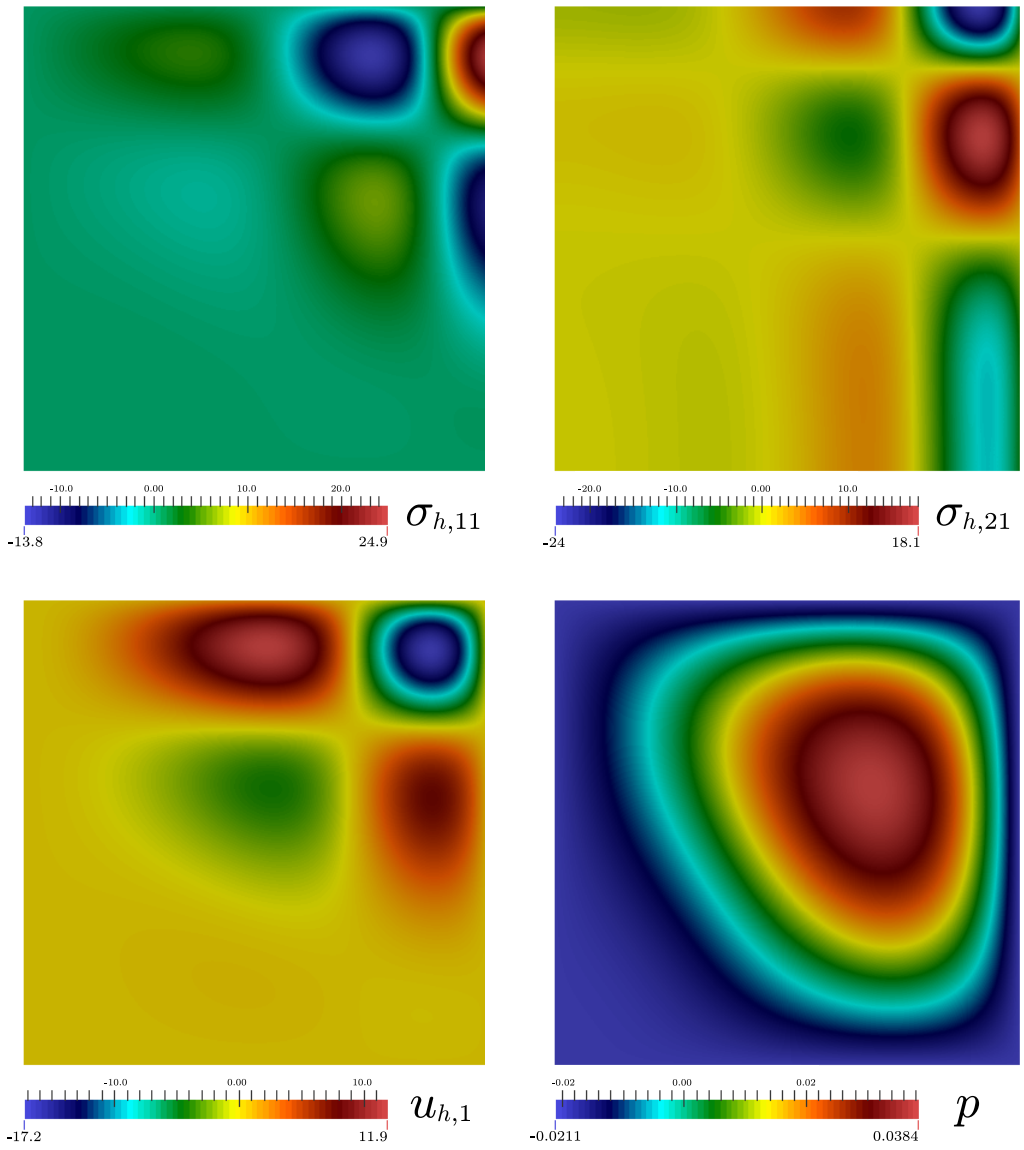

Figure 5.5: Example 1, some components of the approximate solutions ($k = 2$ and $N = 2272302$) using the quasi-uniform scheme.

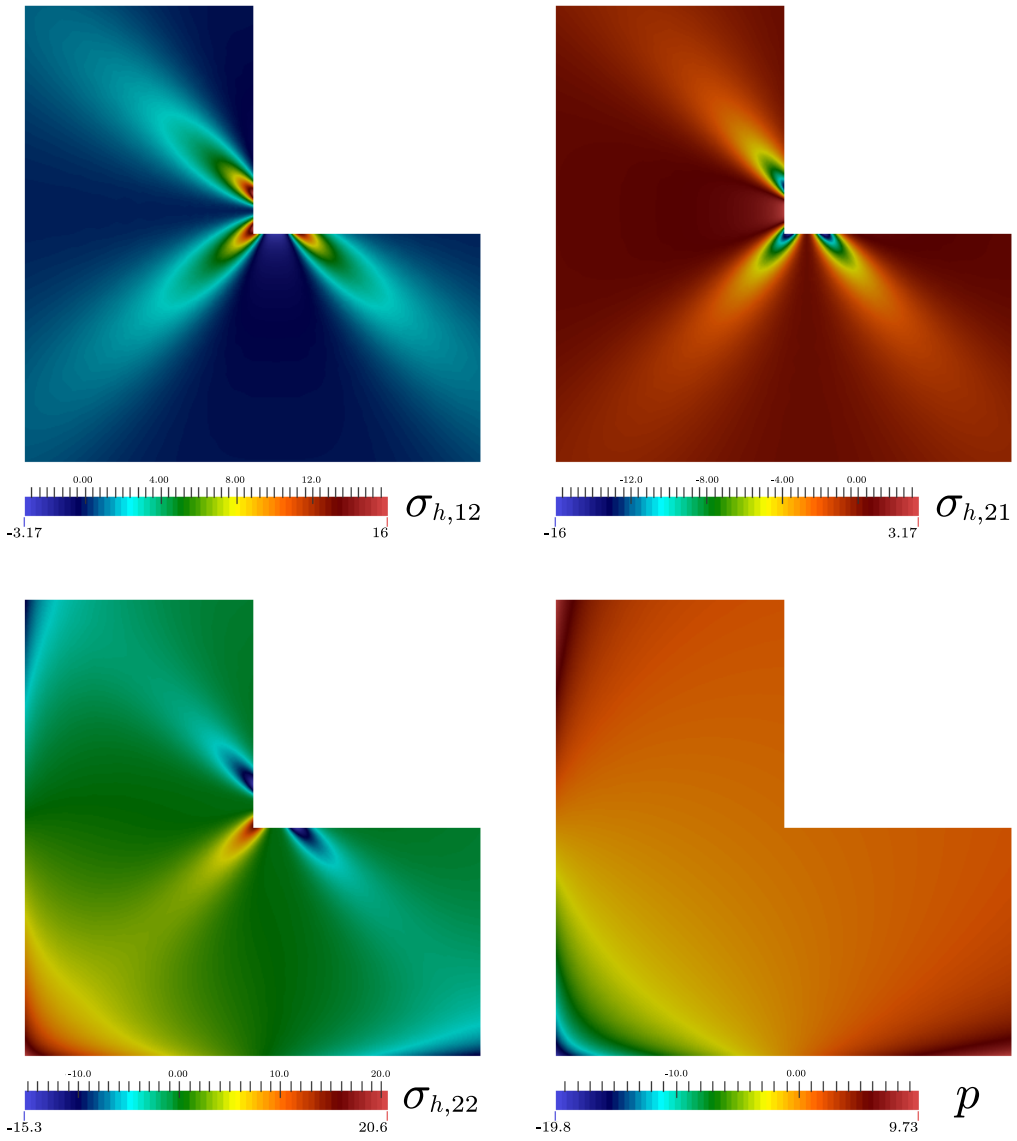

Figure 5.6: Example 2, some components of the approximate solutions ($k = 2$ and $N = 225408$) for the adaptive scheme.

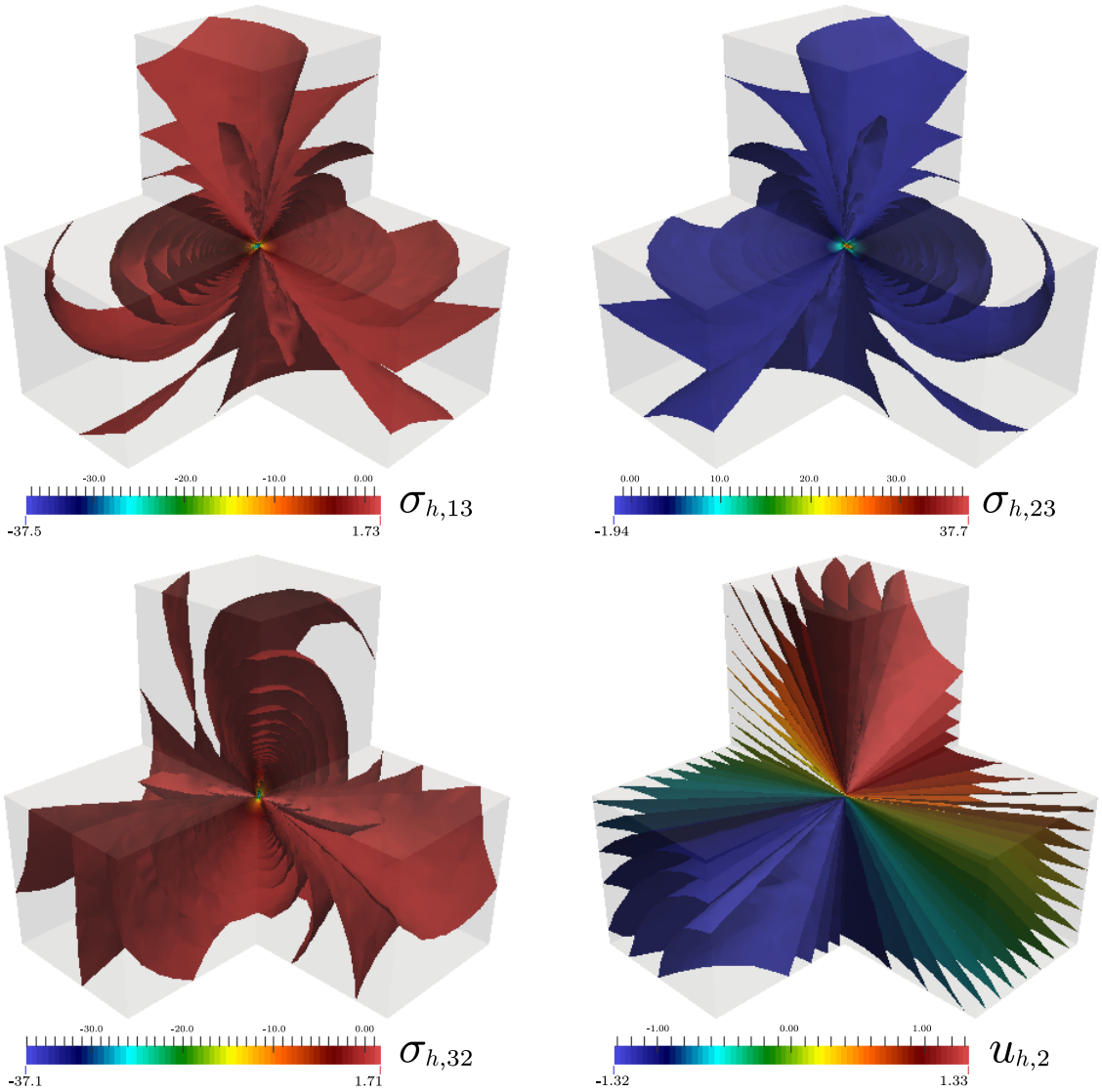

Figure 5.7: Example 3, iso-surfaces of some components of the approximate solutions ($k = 1$ and $N = 1376466$) for the adaptive scheme.